

5

Equilibrium Climate Change - and its Implications for the Future

J. F. B. MITCHELL, S. MANABE, V. MELESHKO, T. TOKIOKA

Contributors:

*A. Baede; A. Berger; G. Boer; M. Budyko; V. Canuto; H. Cao; R. Dickinson;
H. Ellsaesser; S. Grotch; R. Haarsma; A. Hecht; B. Hunt; B. Huntley;
R. Keshavamurty; R. Koerner; C. Lorius; M. MacCracken; G. Meehl; E. Oladipo;
B. Pittock; L. Prahm; D. Randall; P. Rowntree; D. Rind; M. Schlesinger; S. Schneider;
C. Senior; N. Shackleton; W. Shuttleworth; R. Stouffer; F. Street-Perrott; A. Velichko;
K. Vinnikov; D. Warrilow; R. Wetherald.*

CONTENTS

Executive Summary	135	5 3 1 3 Diurnal range of temperature	153
5.1 Introduction	137	5 3 2 Precipitation	153
5 1 1 Why Carry Out Equilibrium Studies ?	137	5 3 3 Winds and Disturbances	153
5 1 2 What are the Limitations of Equilibrium Climate Studies ?	137	5.4 Regional Changes - Estimates for 2030	155
5 1 3 How Have the Equilibrium Experiments Been Assessed ?	137	5 4 1 Introduction	155
5.2 Equilibrium Changes in Climatic Means due to Doubling CO₂	138	5 4 2 Limitations of Simulated Regional Changes	155
5 2 1 The Global Mean Equilibrium Response	138	5 4 3 Assumptions Made in Deriving Estimates for 2030	155
5 2 2 What are the Large-Scale Changes on Which the Models Agree ?	139	5 4 4 Estimates of Regional Change, Pre-industrial to 2030 (IPCC "Business-as Usual Scenario)	157
5 2 2 1 Temperature changes	139	5.5 Empirical Climate Forecasting	158
5 2 2 2 Precipitation changes	143	5 5 1 Introduction	158
5 2 2 3 Soil moisture changes	146	5 5 2 Results	158
5 2 2 4 Sea-ice changes	157	5 5 2 1 Temperature	158
5 2 2 5 Changes in mean sea-level pressure	150	5 5 2 2 Precipitation	158
5 2 2 6 Deep ocean circulation changes	151	5 5 3 Assessment of Empirical Forecasts	158
5.3 Equilibrium Changes in Variability due to Doubling CO₂	152	5.6 The Climatic Effect of Vegetation Changes	159
5 3 1 Temperature	152	5 6 1 Introduction	159
5 3 1 1 Day-to-day variability	152	5 6 2 Global Mean Effects	160
5 3 1 2 Interannual variability	153	5 6 3 Regional Effects Deforestation of Amazonia	160
		5.7 Uncertainties	160
		References	162

EXECUTIVE SUMMARY

1. All models show substantial changes in climate when CO₂ concentrations are doubled, even though the changes vary from model to model on a sub-continental scale.

2. The main equilibrium changes in climate due to doubling CO₂ deduced from models are given below. The number of *'s indicates the degree of confidence determined subjectively from the amount of agreement between models, our understanding of the model results and our confidence in the representation of the relevant process in the model. Five *'s indicate virtual certainties, one * indicates low confidence.

Temperature:

- ***** the lower atmosphere and Earth's surface warm,
- ***** the stratosphere cools;
- *** near the Earth's surface, the global average warming lies between +1.5°C and +4.5°C, with a "best guess" of 2.5°C,
- *** the surface warming at high latitudes is greater than the global average in winter but smaller than in summer (In time dependent simulations with a deep ocean, there is little warming over the high latitude southern ocean);
- *** the surface warming and its seasonal variation are least in the tropics.

Precipitation:

- **** the global average increases (as does that of evaporation), the larger the warming, the larger the increase;
- *** increases at high latitudes throughout the year;
- *** increases globally by 3 to 15% (as does evaporation),
- ** increases at mid-latitudes in winter;
- ** the zonal mean value increases in the tropics although there are areas of decrease. Shifts in the main tropical rain bands differ from model to model, so there is little consistency between models in simulated regional changes;
- ** changes little in subtropical arid areas.

Soil moisture:

- *** increases in high latitudes in winter;
- ** decreases over northern mid-latitude continents in summer.

Snow and sea-ice:

- **** the area of sea-ice and seasonal snow-cover diminish.

The results from models become less reliable at smaller scales, so predictions for smaller than continental regions should be treated with great caution. The continents warm more than the ocean. Temperature increases in southern Europe and central North America are greater than the global mean and are accompanied by reduced precipitation and soil moisture in summer. The Asian summer monsoon intensifies.

3. Changes in the day-to-day variability of weather are uncertain. However, episodes of high temperature will become more frequent in the future simply due to an increase in the mean temperature. There is some evidence of a general increase in convective precipitation.

4. The direct effect of deforestation on global mean climate is small. The indirect effects (through changes in the CO₂ sink) may be more important. However, tropical deforestation may lead to substantial local effects, including a reduction of about 20% in precipitation.

5. Improved predictions of global climate change require better treatment of processes affecting the distribution and properties of cloud, ocean-atmosphere interaction, convection, sea-ice and transfer of heat and moisture from the land surface. Increased model resolution will allow more realistic predictions of global-scale changes, and some improvement in the prediction of regional climate change.

5.1 Introduction

5.1.1 Why Carry Out Equilibrium Studies ?

Climate is in equilibrium when it is in balance with the radiative forcing (Section 3.2). Thus, as long as greenhouse gas concentrations continue to increase, climate will not reach equilibrium. Even if concentrations are eventually stabilised at constant levels and maintained there, it would be many decades before full equilibrium is reached. Thus equilibrium simulations cannot be used directly as forecasts. Why carry out equilibrium studies?

First, approximate equilibrium simulations using atmosphere-oceanic mixed layer models which ignore both the deep ocean and changes in ocean circulation (Section 3, Section 6.4.4.1) require less computer time than time-dependent simulations which must include the influence of the deep ocean to be credible.

Second, equilibrium experiments are easier to compare than time-dependent experiments. This, combined with the fact that they are relatively inexpensive to carry out, makes equilibrium simulations ideal for sensitivity studies in which the effect of using alternative parameterizations (for example, of cloud) can be assessed.

Third, it appears that apart from areas where the oceanic thermal inertia is large, as in the North Atlantic and in high southern latitudes, equilibrium solutions can be scaled and used as approximations to the time-dependent response (see Section 6).

Most equilibrium experiments consider the effect of doubling the concentration of atmospheric carbon dioxide since the effect of increases in other trace gases can be calculated in terms of an effective CO₂ increase (see Section 2). Note that only the radiative effects of increases in gases are taken into account, and not the effects of related factors such as deforestation and possible changes in cloud albedo due to sulphur emissions.

Simulated changes in climate are known to be dependent on the simulation of the undisturbed climate¹ (see, for example, Mitchell et al. 1987). The simulation of present day climate is discussed in more detail in Section 4.

5.1.2 What Are The Limitations Of Equilibrium Climate Studies ?

Firstly, most equilibrium studies use models which exclude possible changes in ocean circulation. Nearly all the equilibrium studies which do allow changes in ocean circulation have been simplified in other ways such as ignoring the seasonal cycle of insolation (Manabe et al., 1990), or using idealised geography (Manabe and Bryan, 1985). The effects of the ocean and the differences between

¹ For example if the snowline is misplaced in the simulation of present climate then the large warming associated with the retreat of the snowline will be misplaced in the simulated climate change.

non-equilibrium and equilibrium climate simulations are discussed further in Section 6.

Secondly, different areas of the world respond at different rates to the gradual increase in greenhouse gases. Over most of the ocean, the response to the increase in radiative heating will be relatively rapid, as little of the extra heat will penetrate below the thermocline at about 500m (see Section 6). On the other hand, in parts of the northern North Atlantic and the high latitude southern ocean, particularly in winter, the extra heat will be mixed down to several kilometres, significantly reducing the rate of warming and consequently the warming reached at any given time. In other words, the geographical patterns of the equilibrium warming may differ from patterns of the time-dependent warming as it evolves in time. This applies both to model simulations and palaeo-climatic analogues.

5.1.3 How Have The Equilibrium Experiments Been Assessed ?

Over 20 simulations of the equilibrium response to doubling CO₂ using general circulation models (GCMs) coupled to mixed-layer oceans have been carried out by 9 modelling groups (Table 3.2a). All those cited involved global models with realistic geography, a mixed layer ocean and a seasonal cycle of insolation. The more recent studies include a prescribed seasonally-varying oceanic heating (Section 3). Models 13, 20 and 21 in Table 3.2a also prescribe a heat convergence under sea ice. Clearly it is not possible here to show results from all 20 or so experiments, so some way of condensing the available data must be chosen. We have chosen not to average the results as there are aspects of each model which are misleading. Nor is it reasonable to choose a 'best' model as a particular model may be more reliable than another for one climatic parameter but not for another. Moreover a result which is common to most models is not necessarily the most reliable - it may merely reflect the fact that many models use similar (possibly erroneous) representations of complex atmospheric processes.

In this section, the climate changes which are common to all models *and which are physically plausible* are emphasised and illustrated by typical results. Where there is disagreement among model results those which are probably unreliable (for example because of large errors in the simulation of present climate) have been eliminated and examples illustrating the range of uncertainty are included. The reasons for the discrepancies (if known) are stated and an assessment of what seems most likely to be the correct result *in the light of current knowledge* including evidence from time-dependent simulations (Section 6), is given.

The contents of the remainder of this section are as follows. First we consider the large-scale changes in

temperature precipitation and other climatic elements in equilibrium simulations of the effect of doubling CO₂, with the emphasis on new results. Several comprehensive reviews have been published recently (for example Dickinson 1986, Schlesinger and Mitchell, 1985,1987, Mitchell 1989) to which the reader is referred for further discussion of earlier studies. The purpose here is to describe the changes and to assess the realism of the mechanisms producing them. The possible changes in climatic variability are then discussed. Next, we consider simulated seasonal mean changes from three different models in five selected regions. These results have been scaled to give a best estimate of the warming which would occur at 2030 (at about the time of effective doubling of CO₂ in the IPCC Business-as-Usual Scenario). This is followed by an assessment of forecasts using the palaeo-analogue method and a review of attempts to model the direct climatic effects of deforestation. Finally, the main uncertainties are discussed.

5.2 Equilibrium Changes in Climatic Means Due to Doubling CO₂

5.2.1 The Global Mean Equilibrium Response

All models show a significant equilibrium increase in global average surface temperature due to a doubling of CO₂ which ranges from 1.9 to 5.2°C (Table 3.2a). Most results lie between 3.5 and 4.5°C, although this does not necessarily imply that the correct value lies in this range. The main uncertainty arises from the problems of simulating cloud. With no changes in cloud a warming of 2 to 3°C is obtained (Table 3.2a, entries 1 and 2 - see also Hansen et al. 1984, Schlesinger 1985) whereas models in which cloud amount is calculated interactively from relative humidity but in which radiative properties are fixed give a warming of 4 to 5°C (Table 3.2a, entries 3 to 16, 21).

Even amongst those models which calculate cloud from relative humidity there is a wide variation in sensitivity (Table 3.2a, entries 3 to 16, 20, 22) and cloud feedback (Cess et al. 1989 - Table 3.2a, entries 3 and 4 - see also Section 3.4.4). Sensitivity also varies for many other reasons including the extent of sea ice in the control climate (Table 3.2a, entries 11 and 12, Manabe and Stouffer 1980, Ingram et al., 1989).

Specifying cloud from relative humidity with fixed radiative properties ignores the possible effects of changes in cloud microphysics, such as changes in total cloud water content, the partition between cloud ice and cloud water, and changes in the effective radius of cloud particles. Because of this, attempts have been made to model cloud water content explicitly (Roeckner et al. 1987, Smith 1990). Climate warming may produce an increase in cloud water content and hence in the reflectivity of cloud (a

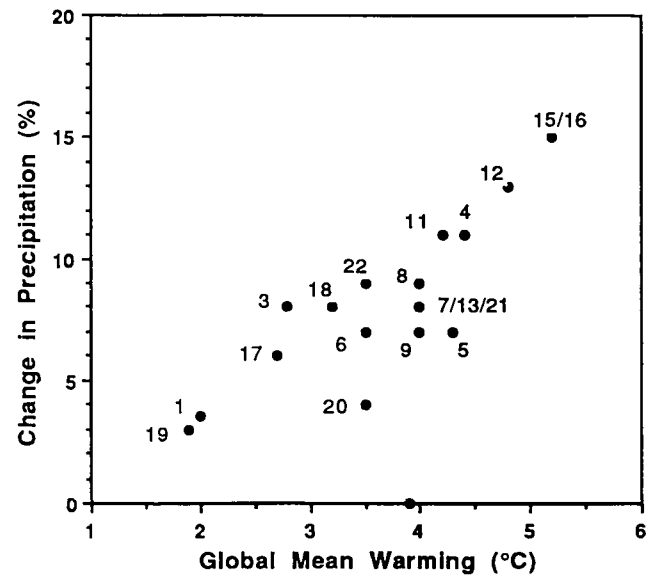


Figure 5.1: Percentage change in globally and annually averaged precipitation as a function of global mean warming from 17 models. The numbers refer to the entries describing the models in Table 3.2a.

negative feedback), but also an increase in the long-wave emissivity of cloud (increasing the greenhouse effect, a positive feedback especially for thin high cloud). Models disagree about the net effect which depends crucially on the radiative properties at solar and infrared wavelengths. One general circulation experiment (Mitchell et al. 1989 - Table 3.2a, entries 18 and 19) and experiments with simple one-dimensional radiative convective models (Somerville and Remer 1984, Somerville and Iacobellis, 1988), suggest a negative feedback. A further possible negative feedback due to increases in the proportion of water cloud at the expense of ice cloud has been identified (Table 3.2a, entries 16, 17, Mitchell et al., 1989).

On the basis of evidence from the more recent modelling studies (Table 3.2a, entries 3, 4, 7-9, 17-22) it appears that the equilibrium change in globally averaged surface temperature due to doubling CO₂ is between 1.9 and 4.4°C. The model results do not provide any compelling reason to alter the previously accepted range 1.5 to 4.5°C (U.S. National Academy of Sciences, 1979, Bolin et al., 1986). The clustering of estimates around 4°C (Table 3.2a, Figure 5.1) may be largely due to the neglect of changes in cloud microphysics in the models concerned. In the 2xCO₂ simulations in which some aspects of cloud microphysics are parameterized (Table 3.2a, entries 17, 20, 22), the warming is less than 4°C. However, in idealised simulations (Cess et al. 1990) changes in cloud microphysics produced positive feedbacks in some models and negative feedbacks in others. Thus we cannot reduce the upper limit

of the range. The modelling studies do not on their own provide a basis for choosing a most likely value.

Dickinson (in Bolin et al., 1986) attempted to quantify the uncertainty in the sensitivity of global mean temperature ΔT_s to doubling CO_2 by considering the uncertainties in individual feedback processes as determined from climate model experiments. The climate sensitivity parameter Λ (the reciprocal of that defined in Section 3.3.1) is the sum of the individual feedback strengths, and the range of ΔT_s is deduced from the range of Λ through

$$\Delta T_s = \Delta Q / \Lambda$$

where ΔQ is the change in radiative heating due to doubling CO_2 (See Section 3.3.1). Repeating this analysis with revised estimates² gives a range of 1.7 to 4.1°C. The mid-range value of Λ gives a sensitivity of 2.4°C which is less than the mid-range value of ΔT_s . This is because for high sensitivity (small Λ), a given increment in Λ gives a bigger change in ΔT_s than for low sensitivity. Similarly, taking the value of Λ corresponding to the middle of the range of Λ implied by 1.5 to 4.5°C gives a value of 2.3°C for ΔT_s .

One can attempt to constrain the range of model sensitivities by comparing predictions of the expected warming to date with observations. This approach is fraught with uncertainty. Global mean temperatures are subject to considerable natural fluctuations (Section 7) and may have been influenced by external factors other than the greenhouse effect. In particular, the effect of aerosols on cloud (Section 2.3.3) may have suppressed the expected warming. There is also some uncertainty concerning the extent to which the thermal inertia of the oceans slows the rate of warming (Section 6). Hence, observations alone cannot be used to reduce the range of uncertainty, though assuming that factors other than the greenhouse effect remain unchanged, they are more consistent with a value in the lower end of the range 1.5 to 4.5°C (Section 8.1.3).

The evidence from the modelling studies, from observations and the sensitivity analyses indicate that the sensitivity of global mean surface temperature to doubling CO_2 is unlikely to lie outside the range 1.5 to 4.5°C. There is no compelling evidence to suggest in what part of this range the correct value is most likely to lie. There is no particular virtue in choosing the middle of the range, and both the sensitivity analysis and the observational evidence

² water vapour and lapse rate feedback $2.4 \pm 0.1 \text{ Wm}^{-2} \text{ K}^{-1}$ (Raval and Ramanathan, 1989); surface albedo feedback $0.3 \pm 0.2 \text{ Wm}^{-2} \text{ K}^{-1}$ (Ingram et al., 1989); cloud feedback $0.3 \pm 0.7 \text{ Wm}^{-2} \text{ K}^{-1}$ (as originally estimated by Dickinson, consistent with range of ΔT_s in Mitchell et al., 1989); the sensitivity $\Lambda = 1.8 \pm 0.7 \text{ Wm}^{-2} \text{ K}^{-1}$ assuming the errors are independent of one another.

neglecting factors other than the greenhouse effect indicate that a value in the lower part of the range may be more likely. Most scientists declined to give a single number but for the purpose of illustrating the IPCC Scenarios, a value of 2.5°C is considered to be the best guess **in the light of current knowledge.**

The simulated global warming due to a doubling of CO_2 is accompanied by increases in global mean evaporation and precipitation, ranging from 3 to 15% (Table 3.2a, Figure 5.1). In general, the greater the warming, the greater the enhancement of the hydrological cycle. Since evaporation increases as well as precipitation, increased precipitation does not necessarily imply a wetter land surface.

5.2.2 What Are The Large-Scale Changes On Which The Models Agree?

Although globally averaged changes give an indication of the likely magnitude of changes in climate due to increases in greenhouse gases, the geographical and seasonal distribution of the changes are needed to estimate the economic and social impacts of climate change. Despite the large range of estimates for the global annual average warming, there are several large-scale features of the simulated changes which are common to all models. These are outlined below. Where appropriate, results from the high resolution models (Table 3.2a, entries 20–22) are quoted to give the reader a rough indication of the size of the changes.

5.2.2.1 Temperature changes

The results from equilibrium simulations shown here are averaged over periods of 5 to 15 years. Because there is considerable interannual variability in simulated surface temperatures, particularly in high latitudes in winter, some of the smaller-scale features may be random fluctuations due to the short sampling period rather than persistent changes due to doubling atmospheric CO_2 .

1. All models produce a warming of the Earth's surface and troposphere (lower atmosphere) and a cooling of the stratosphere (Figure 5.2).

The warming of the surface and troposphere are due to an enhancement of the natural greenhouse effect. The stratospheric cooling is due to enhanced radiative cooling to space and increases with height, reaching 3 to 6°C at about 25 mb. Note that the models considered have at most two levels in the tropical stratosphere and so cannot resolve the details of the stratospheric cooling. Models with high resolution produce a cooling of up to 11°C in the stratosphere on doubling CO_2 (Fels et al., 1980). The indirect effects of stratospheric cooling are discussed in Section 2.2.3. Note that other greenhouse gases (for

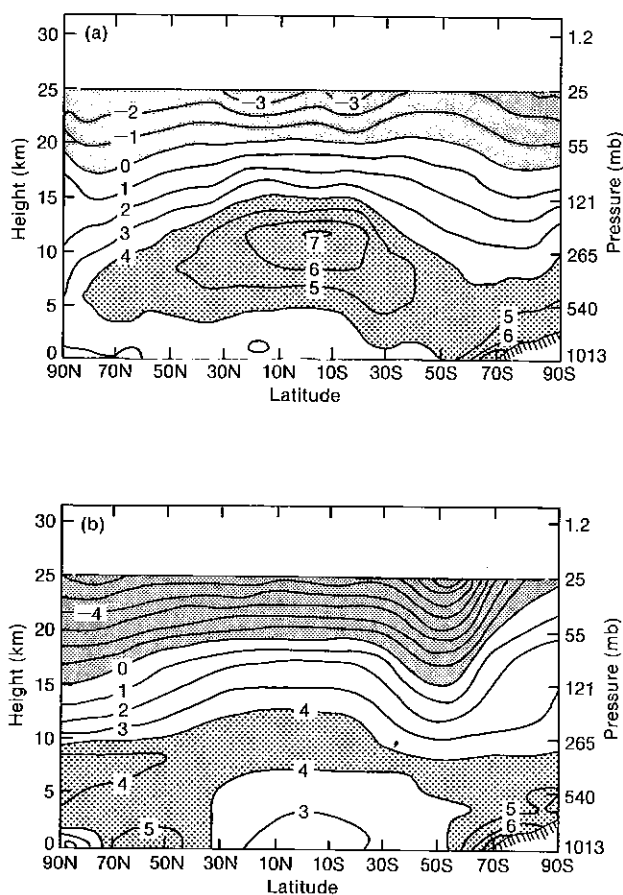


Figure 5.2: Height latitude diagram of the zonally averaged change in air temperature due to doubling CO_2 for the months of June, July and August in two models giving a global mean warming of 4°C . Cooling, and warming by $> 4^\circ\text{C}$, stippled. (from Schlesinger and Mitchell, 1987): (a) with penetrative convection (Hansen et al, 1984), (b) with moist convection adjustment (Manabe and Wetherald, 1988).

example, methane, chlorofluorocarbons) produce a weak radiative warming of the stratosphere (Wang et al., 1990).

2. All models produce an enhanced warming in higher latitudes in late autumn and winter (Figures 5.2, 5.3):

This enhancement of the warming in higher latitudes is the result of a variety of processes.

First, in the warmer $2 \times \text{CO}_2$ climate, sea-ice forms later in autumn giving a pronounced warming in the Arctic (Figures 5.3, 5.4 a, b, c - see over page) and around Antarctica in the corresponding Southern Hemisphere season (Figures 5.3, 5.4 d, e, f - over page). (In high latitudes over the southern ocean, there is little or no warming at any time of year in time-dependent simulations (Section 6)). The reduction in the extent of sea-ice, which is highly reflective, leads to greater solar heating of the surface, mainly in summer, and further warming (a positive "temperature albedo" feedback, see Section 3.3.3). Second,

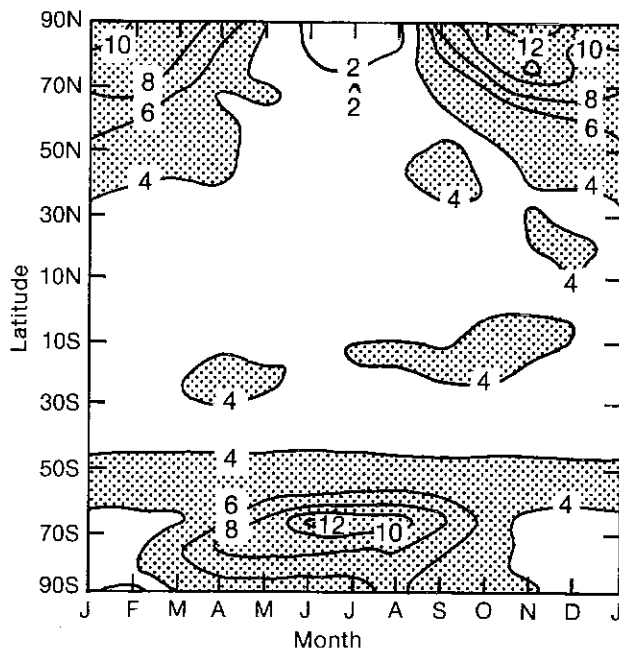


Figure 5.3: Time-latitude diagram of the zonally averaged increase in surface temperature due to doubling CO_2 in the GISS model (Hansen et al, 1984; from Schlesinger and Mitchell, 1987). Warming $> 4^\circ\text{C}$ stippled.

the warming leads to thinner sea ice allowing a greater flux of heat through the ice from the ocean in winter, enhancing the warming of the surface (Manabe and Stouffer, 1980). Third, there is a further temperature albedo feedback over the northern extra-tropical continents in spring due to the reduced extent and earlier melting of highly reflective snow-cover. Fourth, the warming is confined to near the surface. Thus the increase in outgoing long-wave radiation (at the top of the atmosphere) for each degree of warming is small relative to lower latitudes, where the warming is mixed throughout the troposphere. As a result, a larger warming is required in high latitudes to counterbalance the increase in downward radiation due to the increase in greenhouse gases. Finally, there is increased latent-heat release in high latitudes because of the stronger flux of moisture from the tropics (see Section 3).

In the more recent high resolution simulations (Table 3.2a, entries 20 - 22), the warming over North America in winter is about 4°C , rising to 8°C in the northeast of the continent (for example, Figure 5.4 a, b, c - over page). Similarly, over Europe and northern Asia, the warming is of order 4°C , with some areas of much larger warming as for example in eastern Siberia.

The comparatively large warming over sea-ice in autumn and early winter, and over the northern continents in spring, is physically plausible. Much of the variation in these features from model to model can be attributed to

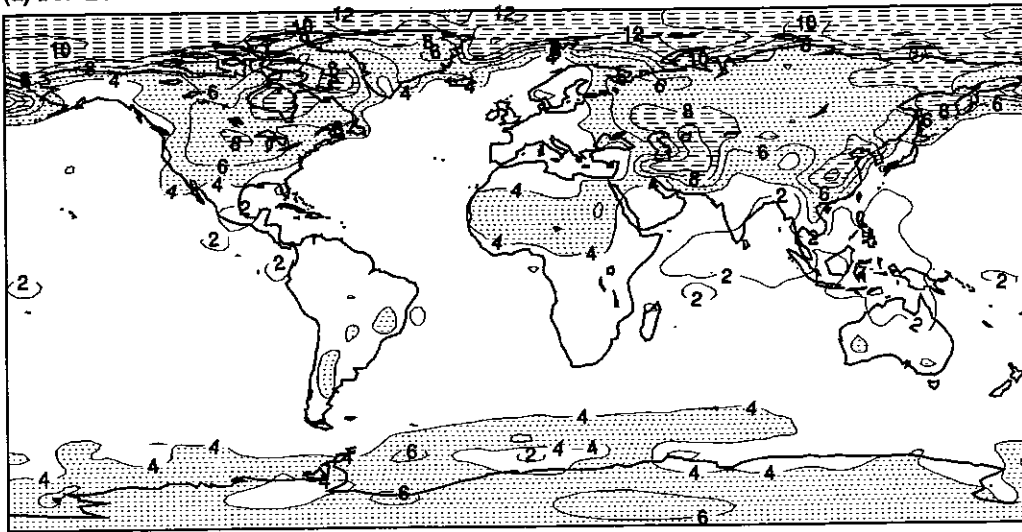
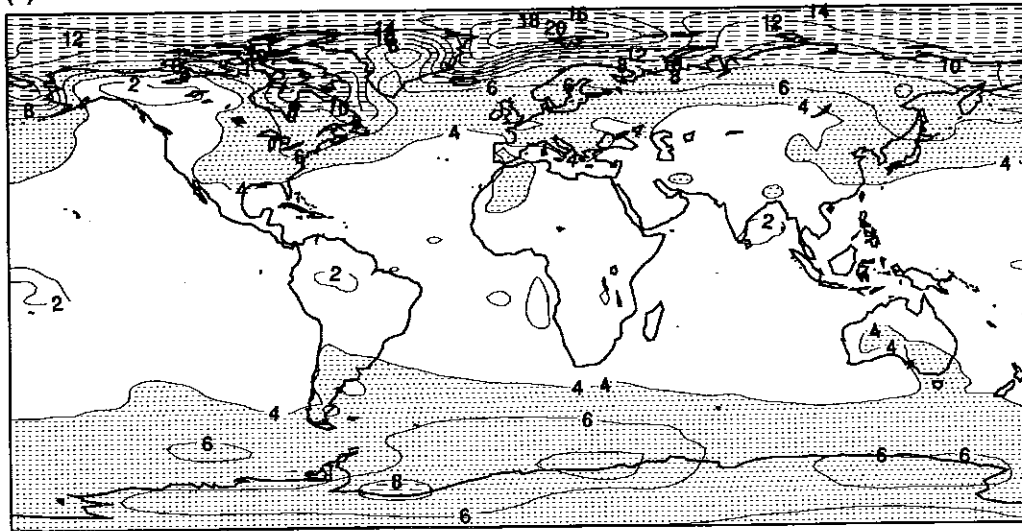
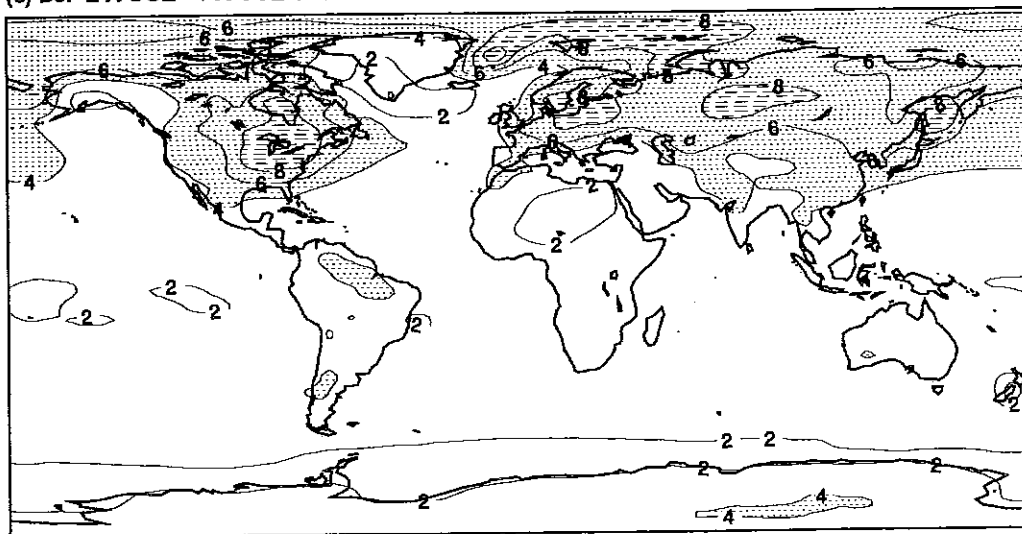
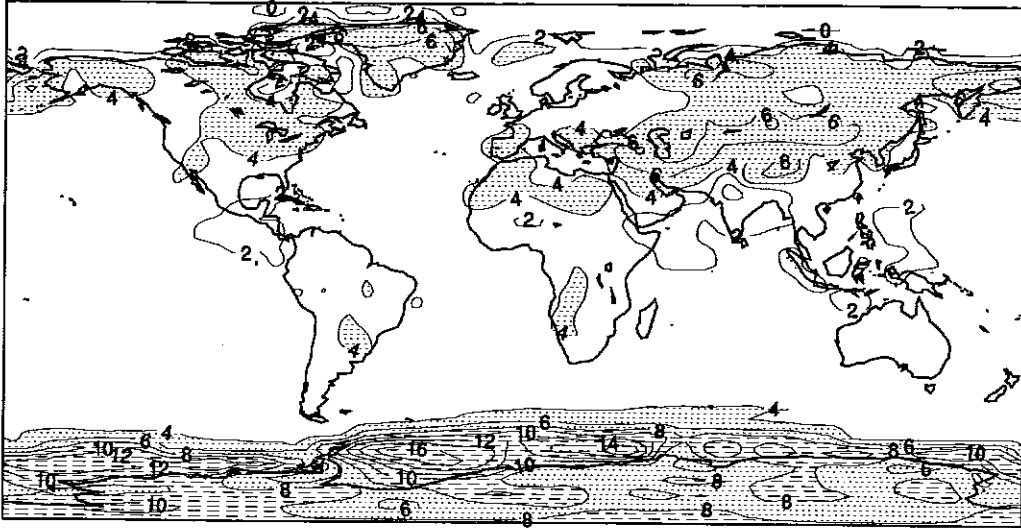
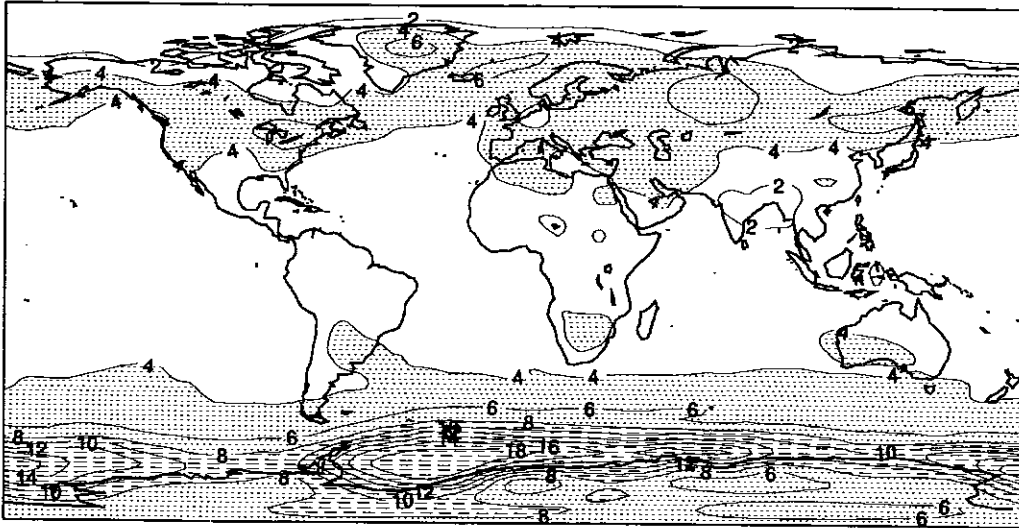
(a) DJF 2 X CO₂ - 1 X CO₂ SURFACE AIR TEMPERATURE: CCC(b) DJF 2 X CO₂ - 1 X CO₂ SURFACE AIR TEMPERATURE: GFHI(c) DJF 2 X CO₂ - 1 X CO₂ SURFACE AIR TEMPERATURE: UKHI

Figure 5.4: Change in surface air temperature (ten year means) due to doubling CO₂, for months December-January-February, as simulated by three high resolution models: (a) CCC: Canadian Climate Centre (Boer, pers. comm., 1989), (b) GFHI: Geophysical Fluids Dynamics Laboratory (Manabe and Wetherald, pers. comm., 1990), and (c) UKHI: United Kingdom Meteorological Office (Mitchell and Senior, pers. comm., 1990). Contours every 2°C, light stippling where the warming exceeds 4°C, dashed shading where the warming exceeds 8°C. Also shown in the colour section.

(d) JJA 2 X CO₂ - 1 X CO₂ SURFACE AIR TEMPERATURE: CCC



(e) JJA 2 X CO₂ - 1 X CO₂ SURFACE AIR TEMPERATURE: GFHI



(f) JJA 2 X CO₂ - 1 X CO₂ SURFACE AIR TEMPERATURE: UKHI

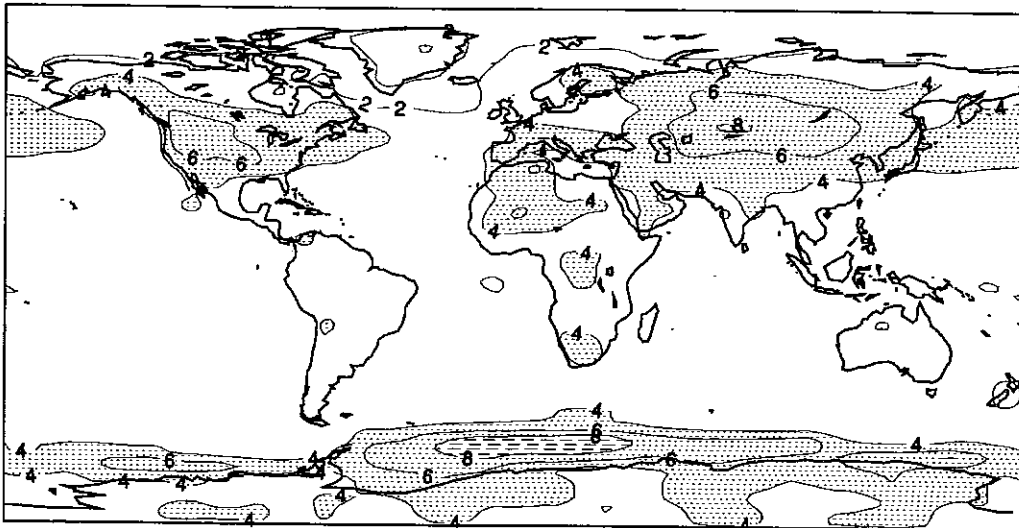


Figure 5.4 continued: Change in surface air temperature (ten year means) due to doubling CO₂, for months June-July-August, as simulated by three high resolution models: (d) CCC, (e) GFHI, and (f) UKHI. Other details as Figure 5.4. Also shown in the colour section.

differences in the sea-ice extents and snow cover in the simulation of present climate.

3. *The warming is smaller than the global mean over sea-ice in the Arctic in summer (Figure 5.4 d, e, f) and around Antarctica in the corresponding season (Figure 5.4 a, c):*

In summer the temperature of the surface of permanent sea-ice reaches melting point in both 1xCO₂ (present day) and 2xCO₂ simulations (Figure 5.3). Even in models where sea-ice disappears in summer in the 2xCO₂ simulation, the large heat capacity of the oceanic mixed layer inhibits further warming above 0°C during the few months when it is ice free. Thus, the winter and annual average warmings are largest in high latitudes, but the summer warming is smaller than the annual average warming.

4. *In all models, the tropical warming is both smaller than the global mean and varies little with season being typically 2 to 3°C (for example, Figures 5.3, 5.4):*

The saturation vapour pressure of water increases non-linearly with temperature, so that at higher temperature, proportionally more of the increase in radiative heating of the surface is used to increase evaporation rather than to raise surface temperature. As a result, the surface warming is reduced relative to the global mean because of enhanced evaporative cooling. The enhanced evaporation is associated with increased tropical precipitation (see Section 5.2.2.2). Thus the warming of the upper troposphere in the tropics is greater than the global mean due to increased latent-heat release (Figure 5.2). Note that the magnitude of the warming in the tropics in those models with a similar global mean warming varies by a factor of almost 2 (Figure 5.2). The reasons for this are probably differences in the treatment of convection (Schlesinger and Mitchell, 1987; Cunningham and Mitchell, 1990) (the vertical transfer of heat and moisture on scales smaller than the model grid), in the choice of cloud radiative parameters (Cess and Potter, 1988) and the distribution of model layers in the vertical (Wetherald and Manabe, 1988). Some of these factors have been discussed further in Section 3.

5. *In most models, the warming over northern mid-latitude continents in summer is greater than the global mean (for example, Figure 5.4 d, e, f):*

Where the land surface becomes sufficiently dry to restrict evaporation, further drying reduces evaporation and hence evaporative cooling, leading to further warming of the surface (Figure 5.5). The reduction in evaporation may also produce a reduction in low cloud (for example, Manabe and Wetherald, 1987), further enhancing the surface warming (Figure 5.5). In one model, (Washington and Meehl, 1984; Meehl and Washington, 1989) the land surface becomes generally wetter in these latitudes in summer, reducing the warming. This is probably due to the

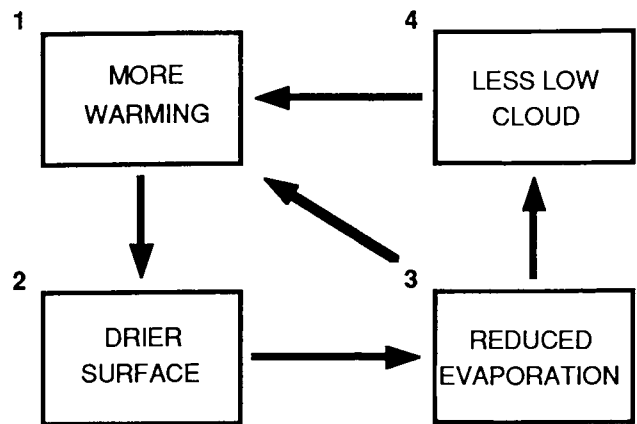


Figure 5.5: Schematic representation of soil moisture temperature feedback through changes in evaporation and low cloud.

land surface being excessively dry in the control simulation (see Section 5.2.2.3).

The summer warming in the more recent simulations (Table 3.2a, entries 20-22) is typically 4 to 5°C over the St. Lawrence-Great Lakes region and 5 to 6°C over central Asia (for example, Figure 5.4 d, e, f). Many of the inter-model differences in the simulated warming over the summer continents can be attributed to differences in the simulated changes in soil moisture and cloud.

5.2.2.2 Precipitation changes

1. *All models produce enhanced precipitation in high latitudes and the tropics throughout the year, and in mid-latitudes in winter (see for example, Figure 5.6):*

All models simulate a substantially moister atmosphere (increased specific humidity). Precipitation occurs in regions of lower level convergence, including the mid-latitude storm tracks and the inter-tropical convergence zone (ITCZ), where moist inflowing air is forced to ascend, cool and precipitate to remove the resulting supersaturation. The increases in atmospheric moisture will lead to a greater flux of moisture into these regions and hence increased precipitation provided there are no large compensational changes in circulation. The high resolution models (Table 3.2a, entries 20-22) give an increase of 10 to 20% in precipitation averaged over land between 35 and 55°N.

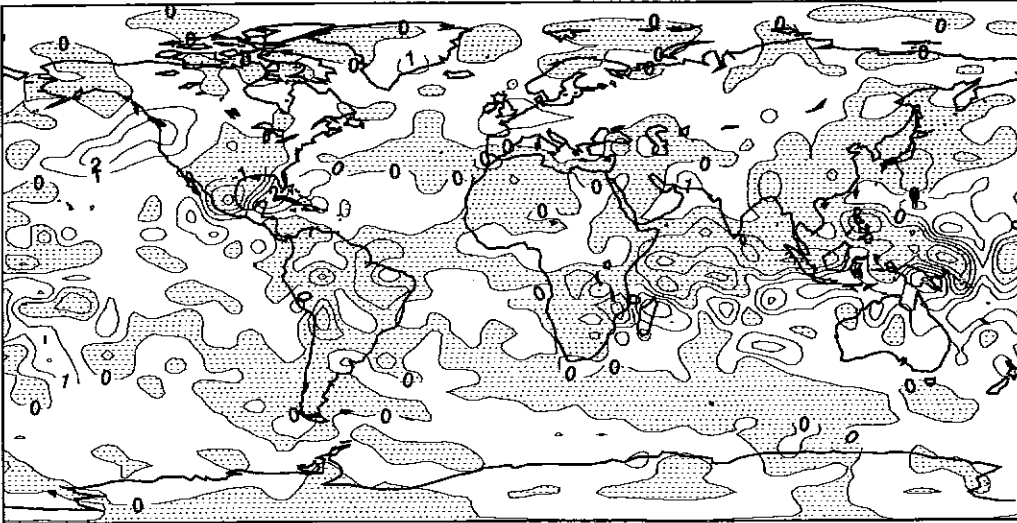
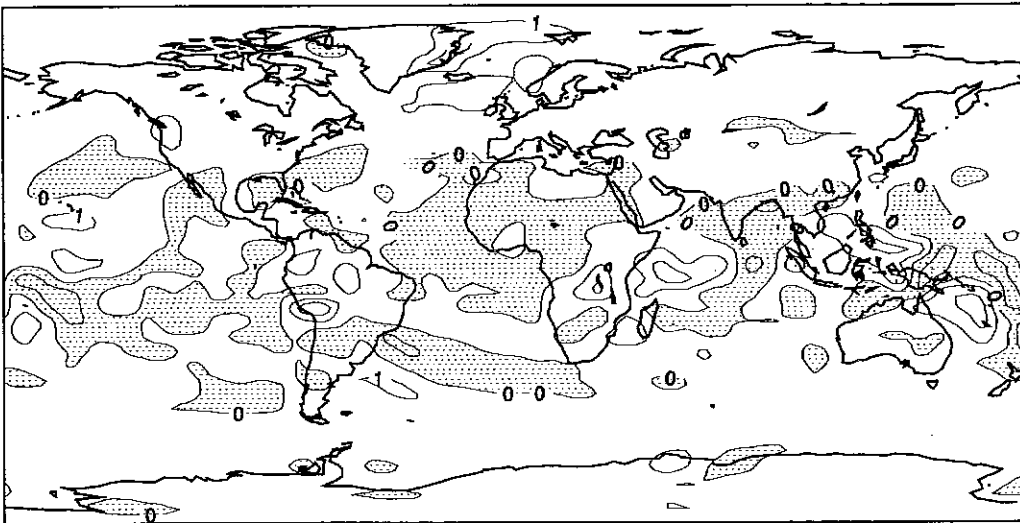
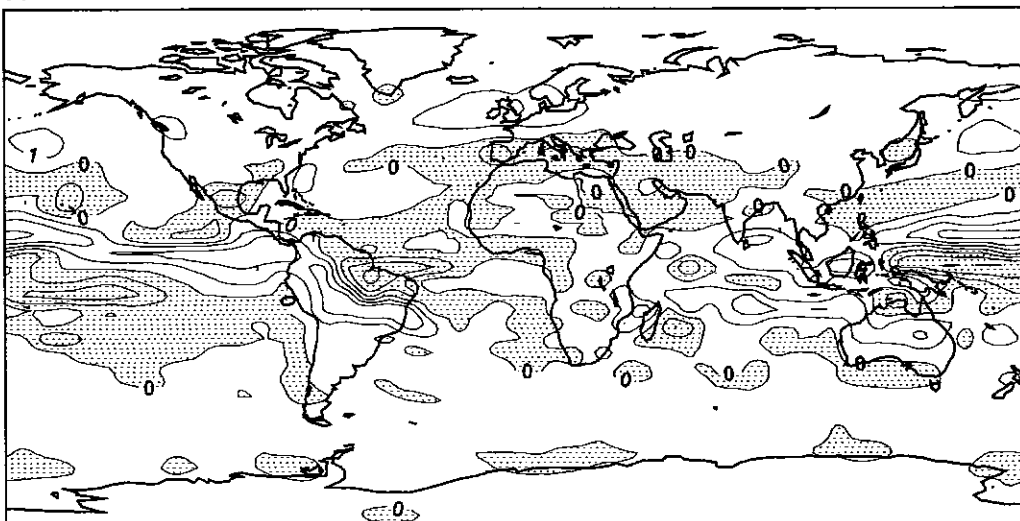
(a) DJF 2 X CO₂ - 1 X CO₂ PRECIPITATION: CCC(b) DJF 2 X CO₂ - 1 X CO₂ PRECIPITATION: GFHI(c) DJF 2 X CO₂ - 1 X CO₂ PRECIPITATION: UKHI

Figure 5.6: Change in precipitation (smoothed 10-year means) due to doubling CO₂, for months December-January-February, as simulated by three high resolution models: (a) CCC, (b) GFHI, and (c) UKHI. Contours at $\pm 0, 1, 2, 5 \text{ mm day}^{-1}$, areas of decrease stippled. Also shown in the colour section.

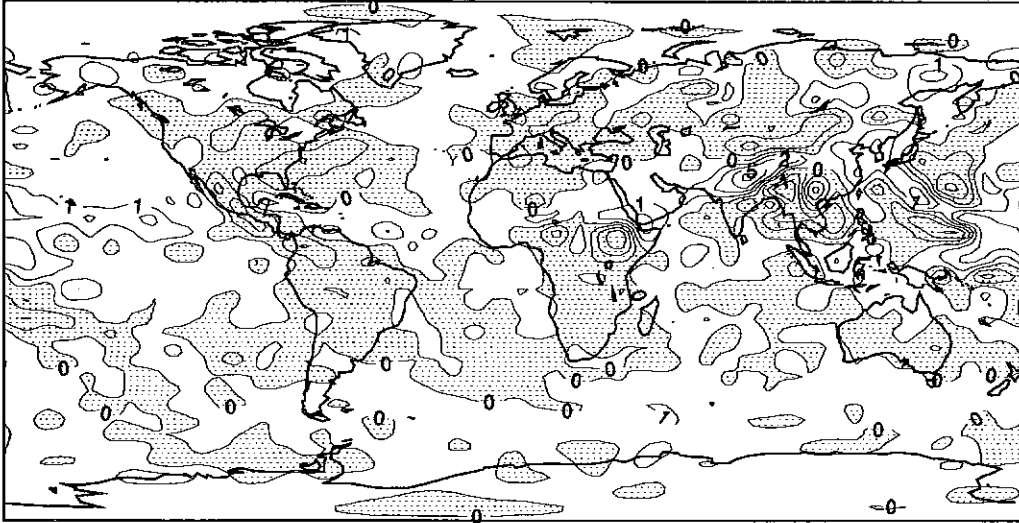
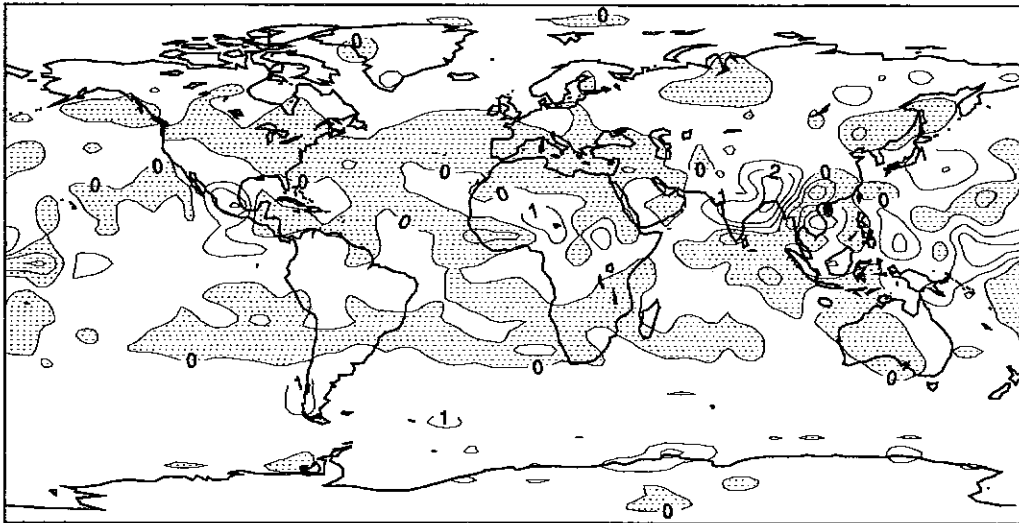
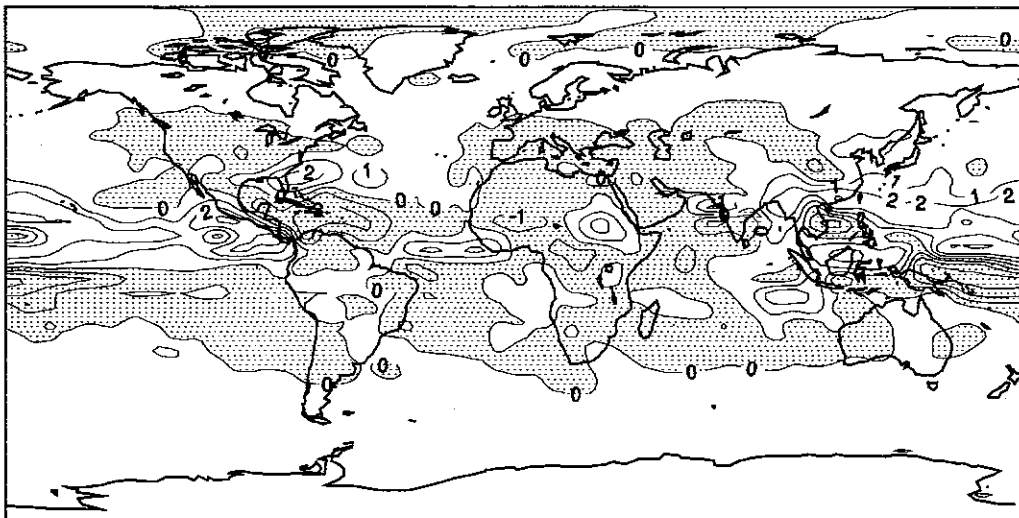
(d) JJA 2 X CO₂ - 1 X CO₂ PRECIPITATION: CCC(e) JJA 2 X CO₂ - 1 X CO₂ PRECIPITATION: GFHI(f) JJA 2 X CO₂ - 1 X CO₂ PRECIPITATION: UKHI

Figure 5.6 continued: Change in precipitation (smoothed 10-year means) due to doubling CO₂, for months June-July-August, as simulated by three high resolution models: (d) CCC, (e) GFHI, and (f) UKHI. Contours at $\pm 0, 1, 2, 5 \text{ mm day}^{-1}$, areas of decrease stippled. Also shown in the colour section.

2. *Changes in the dry subtropics are generally small and with both increases and decreases:*

The interannual variability of precipitation is large relative to its mean value in these regions, so many of the changes indicated by the models cannot be demonstrated to be statistically significant. Note that even small changes of precipitation in arid regions can have substantial impacts.

3. *There are considerable discrepancies regarding changes in precipitation on sub-continental scales, especially in the tropics although most models simulate an enhancement of the precipitation associated with a strengthening of the Southwest Asian monsoon (Table 3.2a, entries 3, 7, 8, 13, 15-22, Figure 5.6):*

The inter-model agreement concerning changes in precipitation is less than in the case of temperature changes for two reasons. First, precipitation is changed indirectly by a wider variety of different processes, many of them not resolved on the model's grid, and so is inherently more difficult to model, whereas the warming is primarily a direct response to increased radiative heating. Second, the changes in precipitation are relatively small compared with the natural variations and so are more difficult to detect in the short sampling period available.

In many of the models, summer rainfall decreases slightly over much of the northern mid-latitude continents and there is a tendency for the tropical maximum of the precipitation to shift further into the summer hemisphere. In other models, the tropical rain belt tends to shift into the winter hemisphere (Table 3.2a, entries 11, 12) or southwards throughout the year (Table 3.2a, entry 6). In some models, enhancement of the Asian monsoon appears to be associated with strong positive cloud feedback whereby decreases in cloud cover over Eurasia in summer enhance the solar heating of the surface (Wilson and Mitchell 1987a). This increases the land-sea temperature contrast which drives the summer monsoon.

Some of the precipitation over mid-latitude continents in summer originates from local evaporation (Mintz, 1984) so the simulated changes in precipitation are likely to be sensitive to the wetness of the surface and the formulation of evapotranspiration. Changes in soil moisture are considered in more detail in the following sub-section.

5.2.2.3 Soil moisture changes.

In all simulations with enhanced CO₂, both evaporation and precipitation increase. In regions where precipitation increases, increases in evaporation may be even greater. Current models represent the availability of water in the upper soil layers by a soil moisture variable, which is augmented by precipitation and snow melt, and depleted by evaporation and runoff. The representations of surface hydrology in models used so far in 2xCO₂ experiments are highly simplified, though some models make allowance for

the type of soil and/or vegetation in a simple manner (Table 3.2a, entries 11, 12, 20). Note that none of the models considered allow for the direct effect of CO₂ on vegetation. Of particular importance is the expected increase in water efficiency (Section 10) which, in the absence of other changes, would reduce evapotranspiration from the surface.

The main findings from equilibrium simulations are:

1. *All models simulate a general increase in the soil moisture of the northern high-latitude continents in winter (Figure 5.7, 5.8 a, b, c):*

This increase is due to some or all of the following factors:- enhanced winter precipitation, more precipitation falling as rain rather than snow, more snowmelt and the relatively low rate of increase of potential evaporation with temperature found at lower winter temperatures. Note only a few models (Table 3.2a, entries 11, 12, 16, 20) allow in any way for the effects of groundwater becoming frozen.

2. *Most models produce an enhanced large-scale drying of the Earth's surface in northern mid-latitude during northern summer (Figure 5.7, 5.8 d, e, f):*

Although there is good agreement among the most recent simulations in this respect, confidence in the reliability of the simulated changes is low in view of the simplified representation of the land surface. In the three high resolution models, the reduction in soil moisture averaged over 35 to 55°N ranges from 17 to 23%. The reasons for this drying are discussed in more detail below. In three of the simulations that do not produce such a drying (Table 3.2a; entries 6, 7, 16), the soil in the control simulation is excessively dry. In the other two (Table 3.2a, entries 11, 12), it has been argued that the simulated changes are equivalent to increased frequency of drought in these latitudes (Rind et al., 1989a).

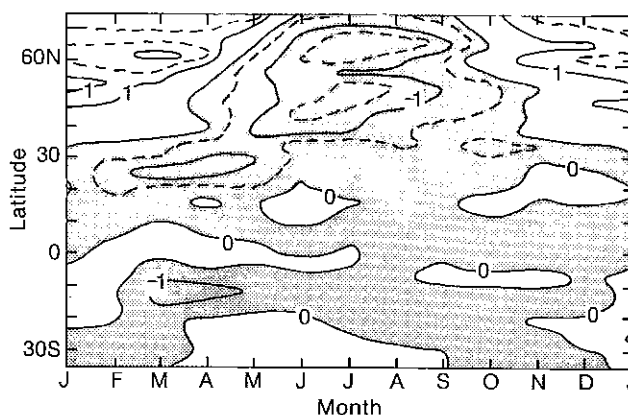


Figure 5.7: Time-latitude diagram of changes in soil moisture due to doubling CO₂. Contours every cm, areas of decrease stippled. (Manabe and Wetherald, 1987).

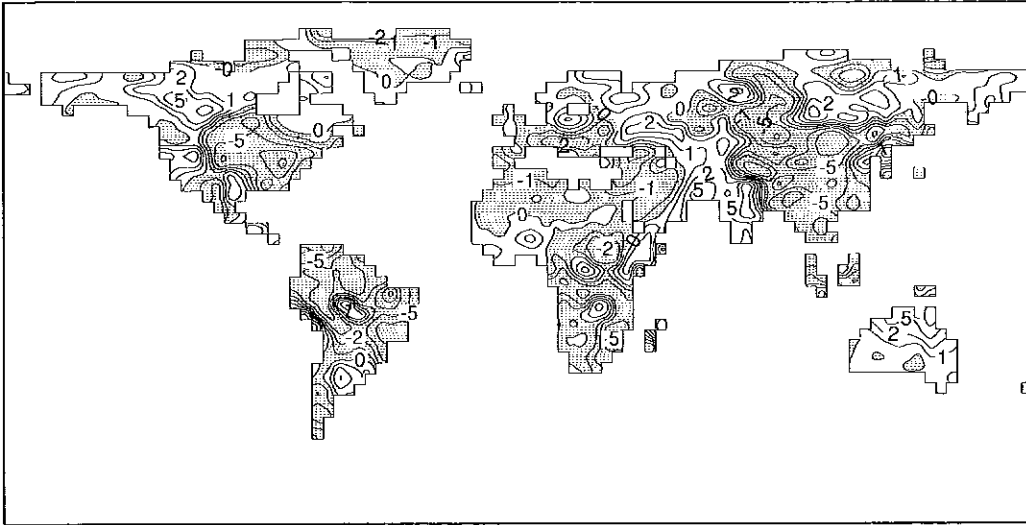
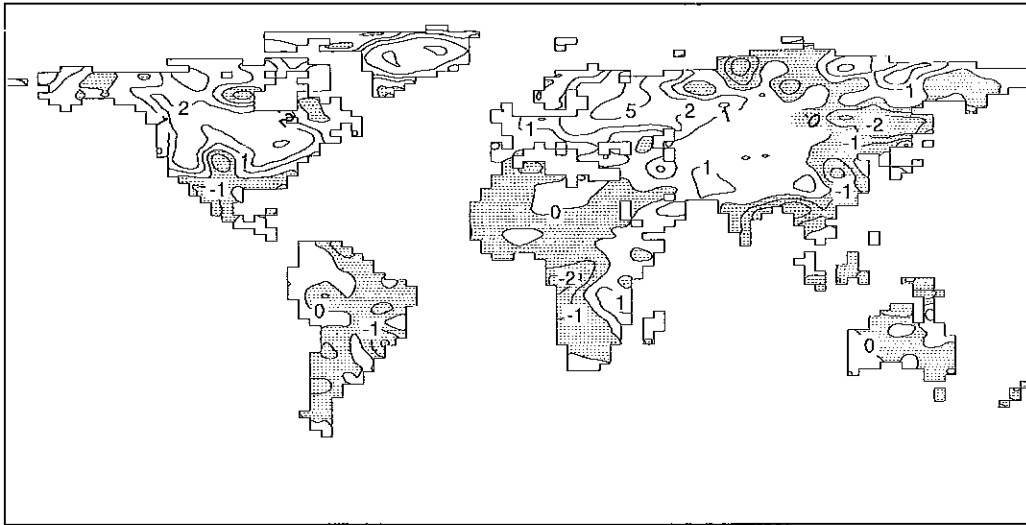
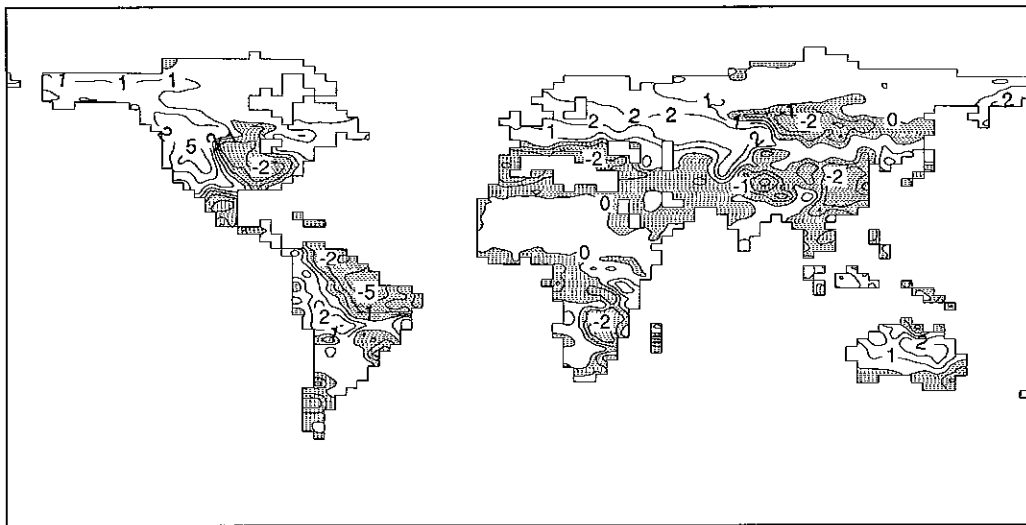
(a) DJF 2 X CO₂ - 1 X CO₂ SOIL MOISTURE: CCC(b) DJF 2 X CO₂ - 1 X CO₂ SOIL MOISTURE: GFHI(c) DJF 2 X CO₂ - 1 X CO₂ SOIL MOISTURE: UKHI

Figure 5.8: Change in soil moisture (smoothed 10-year means) due to doubling CO₂, for months December-January-February, as simulated by three high resolution models: (a) CCC, (b) GFHI, and (c) UKHI. Note that (a) has a geographically variable soil capacity whereas the other two models have the same capacity everywhere. Contours at $\pm 0, 1, 2, 5$ cm, areas of decrease stippled. Also shown in the colour section.

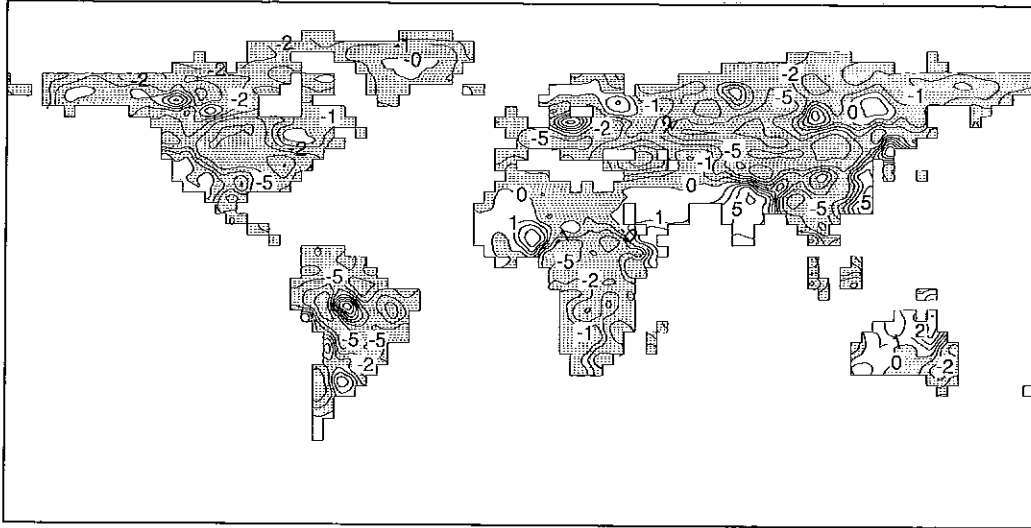
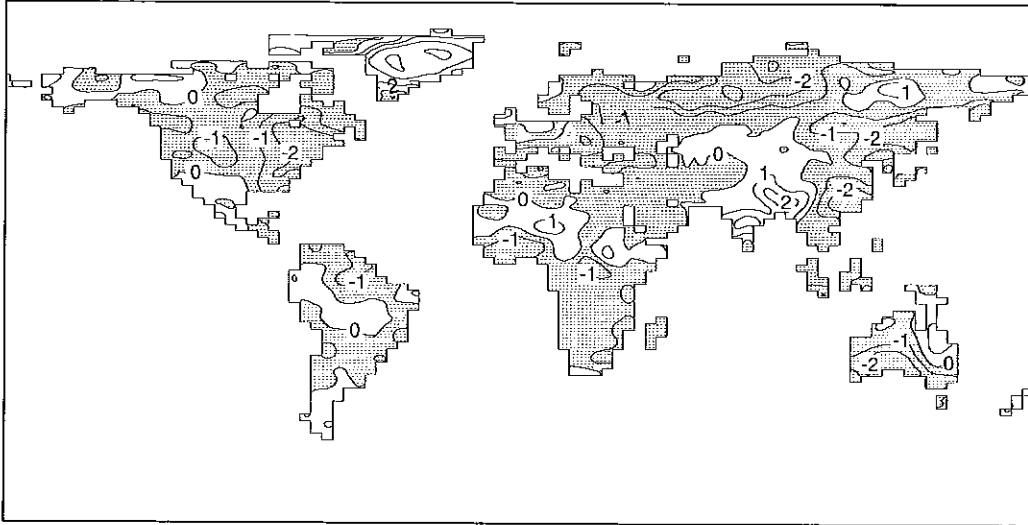
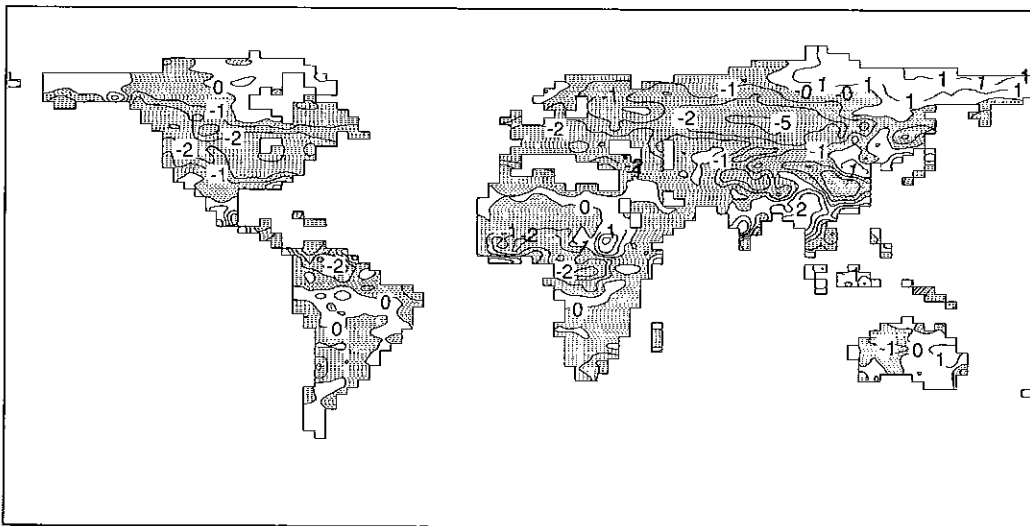
(d) JJA 2 X CO₂ - 1 X CO₂ SOIL MOISTURE: CCC(e) JJA 2 X CO₂ - 1 X CO₂ SOIL MOISTURE: GFHI(f) JJA 2 X CO₂ - 1 X CO₂ SOIL MOISTURE: UKHI

Figure 5.8 continued: Change in soil moisture (smoothed 10-year means) due to doubling CO₂, for months June-July-August, as simulated by three high resolution models: (d) CCC, (e) GFHI, and (f) UKHI. Note that (d) has a geographically variable soil capacity whereas the other two models have the same capacity everywhere. Contours at $\pm 0, 1, 2, 5$ cm, areas of decrease stippled. Also shown in the colour section.

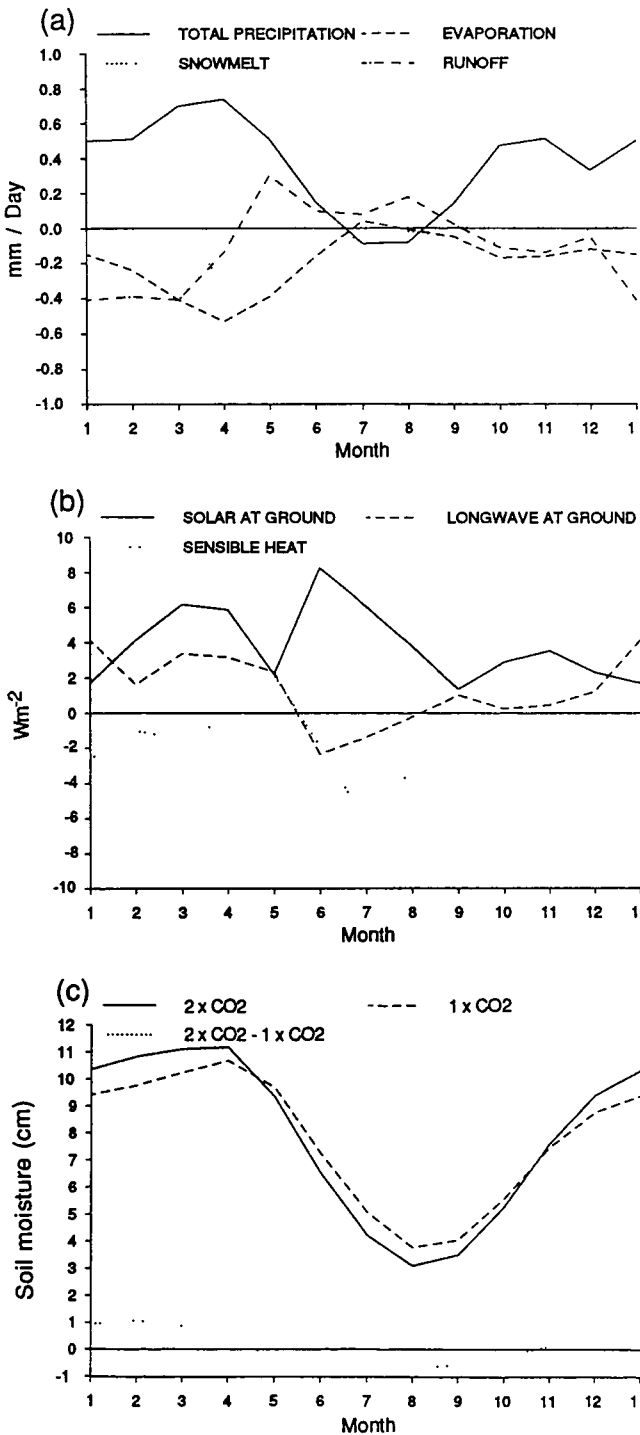


Figure 5.9: Changes in area means due to doubling CO_2 averaged over land between 35 to 55°N . (a) Water budget (mm day^{-1}) (b) Heat budget (Wm^{-2}) (c) Soil moisture ($1\times\text{CO}_2$ and $2\times\text{CO}_2$) (from the study by Manabe and Wetherald, 1987).

Since drying of the northern mid-latitude continents in summer could have significant impacts, these changes warrant a close examination of the physical processes responsible, and the fidelity of their representation in

models needs to be considered carefully. Hence the water and energy budgets in this region have been analysed in some detail. In the control simulation, all models produce a maximum in soil moisture in winter and spring, and a rapid drying to a minimum in summer (Figure 5.9c). With doubled CO_2 , enhanced winter precipitation (and snow melt) (Figure 5.9a) produce higher soil moisture levels into early spring (Figure 5.9c). In the warmer climate, snow melt and the summer drying begin earlier, reducing the soil moisture levels in summer relative to the present climate (Figures 5.8d, e, f, 5.9c). The drying in the $2\times\text{CO}_2$ simulation is also more rapid due to the higher temperatures and in some regions is reinforced by reduced precipitation. Reductions in surface moisture may lead to a drying of the boundary layer, reduced low cloud and hence further warming and drying of the surface (Manabe and Wetherald, 1987) (see also Figure 5.5).

In most models, the soil over much of mid-latitudes (35 to 55°N) is close to saturation in spring in both the $1\times\text{CO}_2$ and $2\times\text{CO}_2$ simulations, so that on enhancing CO_2 , the summer drying starts earlier but from the same level (for example, Figure 5.10a). In a minority of models (Meehl and Washington, 1988, 1989; Mitchell and Warrilow, 1987) the soil in the $1\times\text{CO}_2$ formulation is not close to saturation, and the enhanced winter precipitation in $2\times\text{CO}_2$ simulation is stored in the soil. Hence, although the summer drying in the $2\times\text{CO}_2$ experiments starts earlier, it starts from a higher level than in the control simulation, and may not become drier before next winter season (Figure 5.10b). Even in these models, the surface becomes drier in the southern mid-latitudes in the $2\times\text{CO}_2$ simulations.

From the experiments carried out to date, the following factors appear to contribute to the simulated summer drying in mid-latitudes.

- i) The soil is close to saturation in late winter (spring in higher latitudes) in the control simulation, so that increased precipitation in the anomaly simulation is run off and is not stored in the soil.
- ii) The greater the seasonal variation of soil moisture in the control simulation, the greater the change due to an earlier start to the drying season (for example Figure 5.9c). Of course, if the soil moisture content in the simulation of present climate is very small in summer, it cannot decrease much. A comparison of model and field data over the Soviet Union (Vinnikov and Yeserkepova, 1989) indicates that the simulated soil moisture levels in some models are much too low in summer. The simulated reduction in soil moisture due to doubling CO_2 in such models would then be less than if higher, more realistic levels of soil moisture were present in the control simulation.

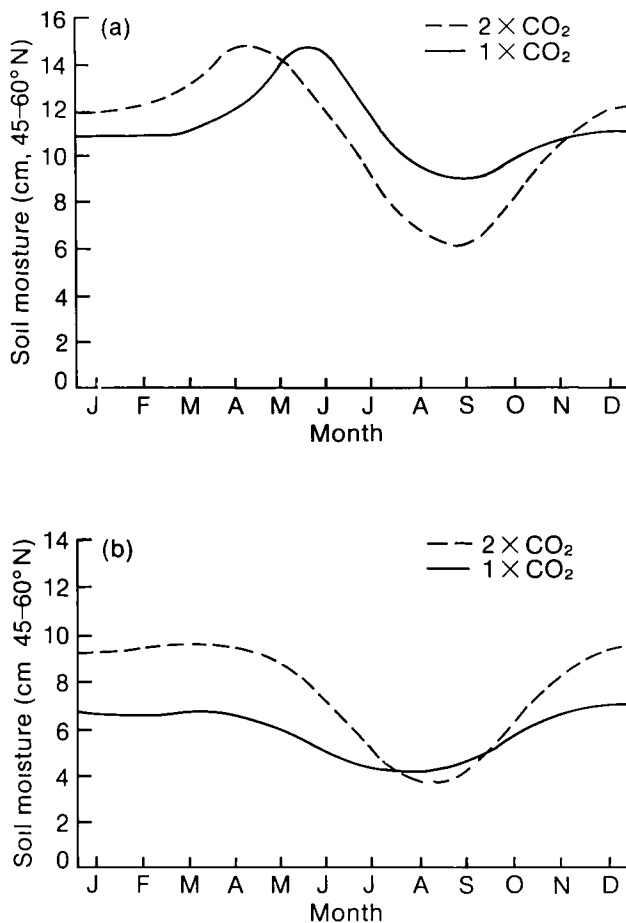


Figure 5.10: Seasonal cycle of soil moisture for normal and doubled CO_2 concentrations, averaged over land, $45\text{--}60^\circ\text{N}$ (a) With standard treatment of runoff (b) With snowmelt runoff over frozen ground (from Mitchell and Warrilow 1987)

- iii) In higher latitudes, snow melts earlier. Hence accurate simulation of snow cover is important.
- iv) The changes in soil moisture can be amplified by feedbacks involving changes in cloud.
- v) Enhanced summer drying in mid-latitudes may occur even in models which produce enhanced precipitation. Of course, the drying is more pronounced in those models (and regions) in which precipitation is reduced in summer.

The simulated changes of soil moisture in the tropics vary from model to model, being more directly related to changes in precipitation.

5.2.2.4 Sea ice changes

In simulations with enhanced CO_2 , both the extent and thickness of sea ice are significantly reduced. In some summer simulations, sea ice is completely removed in the Arctic (Wilson and Mitchell, 1987a; Boer, 1989, personal communication) and around Antarctica (Wilson and Mitchell, 1987a). In other models there are large reductions

in the extent of sea ice but some cover remains in the Arctic and around Antarctica in summer (Noda and Tokioka, 1989; Meehl and Washington, 1989). Finally, in some models (Wetherald, 1989, personal communication) the extent of sea-ice change is less, but the thickness is reduced by up to a factor of two.

The factors contributing to the differences between models include differences in the sea-ice extent and depth in the control simulation (Spelman and Manabe, 1984), differences in the treatment of sea-ice albedo (for example, Washington and Meehl, 1986), and the inclusion of corrective heat-flux under sea ice in some models (for example, Manabe and Wetherald, 1989, personal communication; Boer, 1989, personal communication) and not others.

On the basis of current simulations, it is not possible to make reliable quantitative estimates of the changes in the sea ice extent and depth. It should be noted that the models considered here neglect ice dynamics, leads, salinity effects, and changes in ocean circulation.

5.2.2.5 Changes in mean sea level pressure

Except in areas close to the equator, sea-level pressure (SLP) changes give an indication of changes in the low-level circulation, including the strength and intensity of the mean surface winds. The changes in SLP have been assessed using the limited number of results available (Table 3.2a, entries 7, 13, 15, 20-22), though in most cases, information on the statistical significance of the changes was not provided.

1 Throughout the year there is a weakening of the north-south pressure gradient in the southern hemisphere extratropics (for example, Figure 5.11 over page) implying a weakening of the mid-latitude westerlies.

Both the subtropical anticyclones and the Antarctic circumpolar low pressure trough diminish in intensity (Figure 5.11 over page). This is presumably due to the relatively strong warming over sea-ice around Antarctica, reducing the equator-to-pole temperature gradient (for example, Figure 5.2). Note that at higher levels of the troposphere, the equator-to-pole temperature gradient is increased (for example, Figure 5.2) and may be sufficient to produce **stronger** westerly flow at upper levels (Mitchell and Wilson, 1987a), and that coupled models do not produce a large warming around Antarctica (see Section 6).

2 In December, January, and February most models produce higher pressure off Newfoundland, consistent with an eastward shift of the Iceland low and a general decrease over eastern Siberia, apparently due to a weakening of the Siberian anticyclone (Figure 5.11a).

3 In June, July, and August SLP decreases over Eurasia, intensifying the monsoon low, and there are increases over

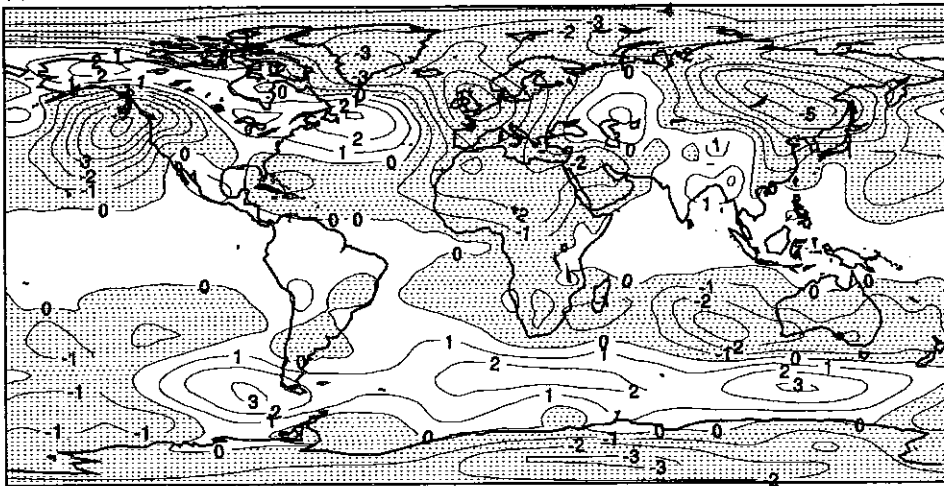
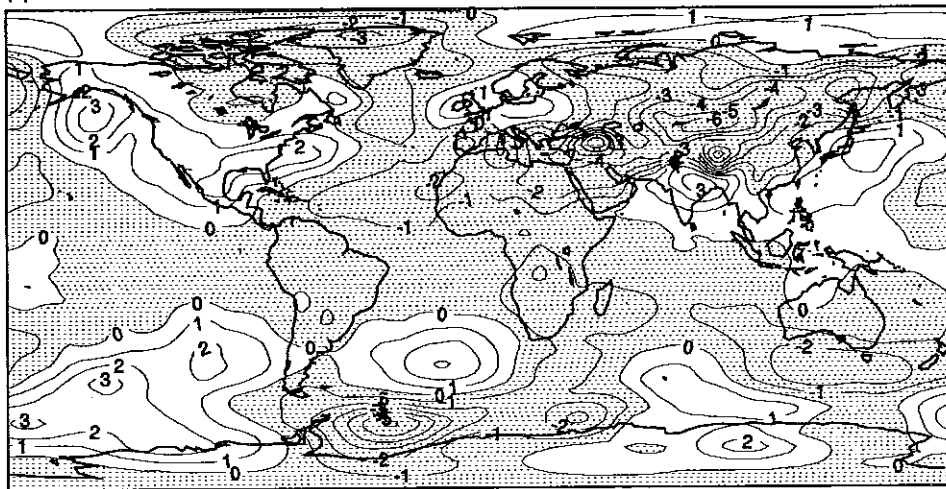
(a) DJF 2 X CO₂ - 1 X CO₂ MEAN SEA LEVEL PRESSURE: CCC(b) JJA 2 X CO₂ - 1 X CO₂ MEAN SEA LEVEL PRESSURE: CCC

Figure 5.11: Changes in mean sea level pressure due to doubling CO₂ as simulated by a Canadian Climate Centre model (Boc, private communication, 1989). Contours every 1 mb, areas of decrease are stippled. (a) December, January and February, (b) June, July and August

India, implying a northward shift of the monsoon trough at those longitudes (Figure 5.11b). There is also a weakening of the Azores anticyclone:

Although these features are common to most of the models considered, there are also large differences in the location of individual features from model to model. Hence changes in low level circulation at a particular location are uncertain. The interannual variability of SLP is large, particularly in the extra-tropics in winter. This, as well as differences in model formulation, contributes to inter-model differences.

5.2.2.6 Deep ocean circulation changes.

There have been few equilibrium CO₂ experiments using atmospheric models coupled to a full dynamical model of the ocean, and most so far (Spelman and Manabe, 1984;

Manabe and Bryan, 1985) have assumed a simplified geometry and neglected the seasonal variation of insolation. Two main features have emerged.

1. The large warming of the ocean in high latitudes is propagated downwards to the ocean floor, where it spreads to all latitudes. The warming of the deep oceans is consistent with palaeo-oceanographic data for a warmer climate (the Cretaceous, about 70 million years ago).
2. There is a weakening of the mean meridional oceanic circulation of the Atlantic on doubling CO₂ from present to higher levels (Manabe et al., 1990). This is also seen in the transient response experiments (Section 6).

5.3 Equilibrium Changes in Variability due to Doubling CO₂

Changes in the variability and frequency of extreme events may have more impact than changes in mean climate. Changes in the frequency of extreme events may occur in a number of ways. For example, the shape of the frequency distribution may not be altered, but the mean may change, leading to a sharp increase in the frequency of extreme events at one end of the frequency distribution, and a decrease at the other end (Mearns et al., 1984,1990; Parry and Carter, 1985; Wigley, 1985; Pittock, 1989) (Figure 5.12a). Thus the general warming due to increases in greenhouse gases will undoubtedly lead to more frequent "hot" days and fewer "cold" days. Conversely, the mean may be unchanged, but the shape of the frequency distribution may alter. For example, the standard deviation (spread) of the frequency distribution may increase producing more extreme events at both ends of the distribution (Figure 5.12b). Of course, the mean and the spread of the frequency distribution may change simultaneously.

In the first example, the changes in the frequency of extreme events can be calculated by simply shifting the currently observed (or simulated control) frequency distribution by the mean change (Figure 5.12a). Here, the second type of change is considered in more detail. The standard deviation of the frequency distribution is used as a measure of variability, and both the standard deviation of daily values about the monthly mean and the standard deviation of the interannual variation of monthly means are considered, as appropriate. For day-to-day variability, results from only two models were available (Table 3.2a, entries 20, 22), whereas for interannual variability, results

from five models were used (Table 3.2a, entries 7, 11, 13, 15, 20).

Several factors must be borne in mind when deriving changes in standard deviations from numerical simulations. First, a much longer simulation is required to establish that changes in standard deviations, as opposed to changes in means, are statistically significant. Most studies to date use periods of 15 years or less, which is barely sufficient to establish that the simulated changes in standard deviation are unlikely to have occurred by chance. Second, although the models exhibit a measure of agreement on the larger scales, there is much less agreement on the regional scale, especially in the case of precipitation. Hence, only the changes in standard deviations on the larger scales will be considered. Third, information on changes in variability is not as readily available as information on changes in means. Thus the conclusions below are based on a much smaller number of simulations than is generally the case in Section 5.2. Finally, the coupled atmosphere mixed layer models used to derive the results in this section do not reproduce the El Niño - Southern Oscillation phenomena which are the main source of interannual variability in the tropics (Section 7.9.1).

5.3.1 Temperature

5.3.1.1 Day-to-day variability

Results from only two models were available globally. There are reductions in the standard deviation over and around the winter sea-ice margins - notably over Hudson Bay, the Norwegian Sea and the Sea of Okhotsk in January and around Antarctica in July. The decrease in these regions may be attributed to the reduction in the north-south temperature gradient (Figure 5.4), and to a reduction

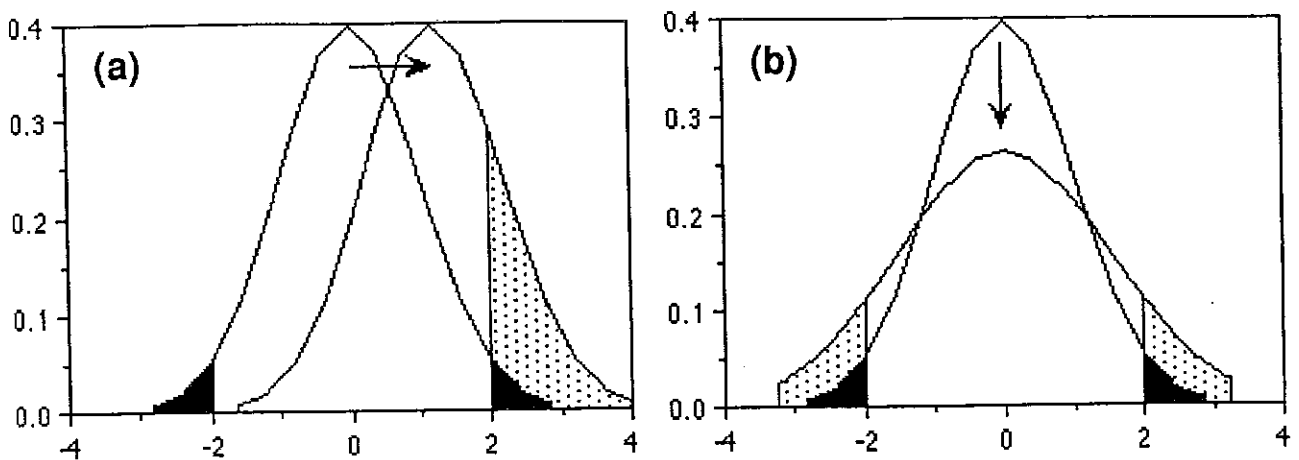


Figure 5.12: Schematic changes in frequency distributions. The solid area marks the 5% extremes of a normal distribution. The shaded area represents an increase in the number of extreme events outside the unperturbed 5% limits. (a) Increase in mean only. Note the large increase in the number of extreme events to the right of the original distribution, (b) No change in mean but a 50% increase in standard deviation. Note the increase in extreme events on both sides of the original distribution.

in the frequency or intensity of atmospheric disturbances (see Section 5.3.3). There are also reductions over much of the northern hemisphere continents in January, although both models produce increases over parts of Canada and Siberia. A third study (Rind et al., 1989b) reports decreases over the United States though generally they are not statistically significant.

5.3.1.2 *Interannual variability*

Apart from a general reduction in the vicinity of the winter sea-ice margins, no meaningful patterns of change could be distinguished (Five models were considered, Table 3.2a, entries 7, 11, 13, 15, 20).

5.3.1.3 *Diurnal range of temperature*

There is no compelling evidence for a general reduction in the amplitude of the diurnal cycle.

The increases in CO₂ and other greenhouse gases increase the downward longwave flux at the surface (Section 2). Both the upward flux of longwave radiation and evaporative cooling increase non linearly with surface temperature. One would expect the increased downward radiation to produce a larger warming at night (when the surface temperature and hence the rate of increase of radiative and evaporative cooling with increase in temperature is smaller) than during the day and hence a reduction in diurnal range.

Only a few models contain a diurnal cycle (see Table 3.2a). Boer (personal communication) reports a small reduction (0.28°C) in the globally averaged diurnal range of temperature (Table 3.2a, entry 20). In another study (Rind et al., 1989b) the range usually decreased over the United States, especially in summer. However Cao (personal communication) found that increases in the diurnal range of temperature were evident over much of the northern mid-latitude continents especially in spring and autumn (Table 3.2a, entry 15) although the global annual mean was reduced by 0.17°C. The amplitude of the diurnal cycle may also be reduced by increases in cloud cover or ground wetness, or altered by changes in the latitude of the snowline. As these quantities (and changes in these quantities) vary greatly from model to model a reduction in the diurnal cycle seems far from certain.

5.3.2 *Precipitation*

Precipitation exhibits much more temporal and spatial variability than temperature. As a result, the simulation of the mean (and variability) of precipitation for present day climate is less reliable than for temperature, particularly in low resolution models, and it is only possible to make weak statements concerning changes in variability.

1 There is some indication that variability (interannual standard deviation) increases where mean precipitation

increases and vice-versa (Wilson and Mitchell 1987b Rind et al. 1989b), though this is not always the case

For example, in one study (Rind et al., 1989b) this tendency in interannual variability was found at 60-70% of the grid-points considered. In another study (Wilson and Mitchell, 1987b) the summer rainfall over southern Europe decreased and the maximum number of consecutive days without rainfall increased substantially.

2 There is a consistent increase in the frequency of convective (sub grid-scale) precipitation usually at the expense of precipitation from the larger scale (resolved) vertical motions (Noda and Tokioka 1989 Hansen et al. 1989 Mitchell pers comm)

In one study (Noda and Tokioka, 1989) the area of precipitation over the globe decreased even though global mean precipitation increased. There is a tendency for convective motions to penetrate higher (Mitchell and Ingram, 1989, Wetherald and Manabe, 1988) and perhaps over greater depth (Hansen et al., 1989) in a warmer climate. These changes imply an increase in the more intense local rain storms and hence in run off, at the expense of the gentler but more persistent rainfall events associated with larger scale disturbances. Note that not all models include the diurnal cycle which has a strong modulating influence on convection.

The tendency for local convective instability to increase is likely to be independent of the particular model used as in a warmer climate, the radiative cooling of the atmosphere and the radiative heating of the surface both increase (Mitchell et al., 1987). These changes must be balanced by the enhanced vertical transport of heat from the surface. Furthermore, given the non-linear increase in potential evaporation with increase in temperature the increase in vertical heat transport is more likely to be achieved through latent heat rather than by sensible heat, and hence accompanied by a marked increase in convective rainfall.

5.3.3 *Winds and Disturbances*

Current climate models particularly those at lower resolution have limited success in simulating storm tracks and low frequency variability, and do not resolve smaller scale disturbances such as hurricanes explicitly (Sections 4.2.4, 4.6). Hence results from current models at best only give an indication of the likely changes in winds and disturbances.

1 There is some indication of a general reduction in day to day and interannual variability in the mid-latitude storm tracks in winter though the patterns of change vary from model to model

Here, the standard deviation of variations in mean sea-level pressure (SLP) has been used as an indication of the

frequency and intensity of disturbances. A reduction in mid-latitude synoptic variability might be expected as a result of the reduction in the equator to-pole temperature gradient at low levels (for example Figure 5.2). Results on changes in day-to-day variability were available from only two models. There was a general reduction in the standard deviation in mid-latitudes in winter though the patterns of change differed considerably. By applying a time filter to the daily variances of 500mb height one can pick out the mid latitude storm tracks (Blackmon 1975). In winter Siegmund (1990) found a reduction in the intensity of the filtered variances of 500mb height in mid latitudes and an increase in high latitudes (Table 3.2a entry 15). In another study (Bates and Meehl 1986 Table 3.2a entry 6) a similar reduction in the filtered variance of 500mb heights was reported. All these changes indicate a decrease in the intensity or frequency (or both) of disturbances resolved on the model grid (typically greater than about 1 000 km) but do not allow one to conclude the same for smaller scale synoptic disturbances. One study (Bates and Meehl 1986) reports a reduction in blocking (defined as areas of high pressure anomaly which persist for more than seven days) in the southern hemisphere, and changes in the positions but not the intensity of blocking in the Northern Hemisphere though no information was provided on the statistical significance of the results.

In the five models considered there was a general reduction in the standard deviation of interannual variations in monthly mean SLP. However the patterns varied considerably from model to model so no other meaningful conclusions could be drawn.

2. There is some evidence from model simulations and empirical considerations that the frequency per year intensity and area of occurrence of tropical disturbances may increase though it is not yet compelling.

It has been observed that tropical storms (hurricanes typhoons or cyclones) form only where the sea surface temperatures (SSTs) are 27°C or greater. This might lead one to expect a more widespread occurrence of tropical storms in a warmer climate. A recent theoretical model of tropical storms suggests that the maximum possible intensity would increase, with an enhancement of destructive power (as measured by the square of the wind speed) of 40% for an increase of 3°C in SST (Emanuel 1987). However, Emanuel (1987) did note that very few tropical storms in the present climate actually attained the maximum intensity predicted by his analysis. In a complementary study, Merrill (1988) discussed the environmental influences on hurricane intensification. In agreement with Emanuel Merrill concluded that the maximum intensity of a tropical storm is bounded above by a monotonically increasing function of sea surface temperature (SST). By compositing intensifying versus

non intensifying systems over a six year period for the North Atlantic Merrill was able to identify a number of environmental factors which could inhibit the further deepening of a tropical storm, even if the SSTs are favourable. The non intensifying composite storms displayed stronger vertical wind shears and uni directional flow over and near the storm centre than intensifying storms. Gray (1979) identified the need for weak vertical wind-shear over and near the storm centre and enhanced low-level cyclonic vorticity and mid-tropospheric humidity as factors favouring intensification of a tropical cyclone. There is no guarantee that criteria such as the lower bound of SST of 27°C would remain constant with changes in climate. There is little agreement in the simulated changes in tropical circulation due to doubling CO₂ in current climate models (as shown by the differing patterns of changes in tropical precipitation). Furthermore, the models considered in this section ignore changes in ocean circulation which form part of the El Niño phenomenon and lead to the associated anomalies in SST and atmospheric circulation which have a profound influence on the present distribution and frequency of tropical storms.

High resolution atmospheric models used for weather forecasting show considerable success at predicting the development and track of tropical cyclones (Dell Osso and Bengtsson 1985 Krishnamurti et al., 1989, Morris 1989) although the horizontal resolution used (~100km) is inadequate to resolve their detailed structure. Krishnamurti et al. (1989) found that the quality of the forecasts decreased as horizontal resolution was decreased but even so the simulated maximum wind intensity decreased little until much coarser (above 400 km) resolution was reached. At the lower resolution used in climate studies (250 km or greater) one can choose objective criteria (for example, a warm core and low level vorticity and surface pressure depression greater than specified limits) to select appropriate cyclones and compare their seasonal and geographical distributions with those of observed tropical storms. In both respects the simulated storms resemble those observed over most oceans (Manabe et al. 1970, Bengtsson et al. 1985 Broccoli and Manabe 1990 (Table 3.2a entry 21)). Thus although global models cannot resolve hurricanes explicitly they give a surprisingly good indication of the regions of potential hurricane formation. In contrast to empirical methods the criteria chosen are not obviously dependent on the present climate.

Using models with prescribed cloudiness, Broccoli and Manabe (1990) found an increase of 20% in the number of storm days (a combined measure of the number and duration of storms) on doubling CO₂. This is attributed to enhanced evaporation leading to increased moisture convergence and latent heat release which is converted to locally transient kinetic energy (stronger winds). In

contrast, in an experiment in which cloudiness was allowed to change, the number of storm days decreased by 10 to 15% even though the increase in evaporation was even greater in this experiment. The increases in local energy generation and conversion were smaller, and the associated winds weakened slightly. The reason for this discrepancy has not been found, nor has the role of cloud feedback in these results been identified.

A preliminary experiment with a model which resolves hurricanes (Yamasaki, personal communication) showed an increase in the number, and a decrease in the intensity of tropical disturbances when sea surface temperatures were increased, but the simulation was very short.

In summary, the maximum intensity of tropical storms may increase, but the distribution and frequency of occurrence will depend on the detailed changes in aspects of circulation in the tropics which are probably not yet adequately simulated by climate models.

5.4 Regional Changes - Estimates for 2030 (assuming IPCC "Business-as-Usual" Scenario)

5.4.1 Introduction

In order to assess the impacts of future changes in climate, one needs to know the changes and rates of change in climate on a regional scale (i.e., areas of order 1000 km square or so). Results from current equilibrium experiments often differ regarding regional variations in the changes. Furthermore, few time-dependent simulations have been carried out (Section 6), none correspond exactly to the IPCC Scenarios and all use low horizontal resolution. Nevertheless, one of the briefs of Working Group I was to provide estimates of changes in 5 selected regions.

In order to provide these regional estimates it has been necessary to make certain assumptions and approximations (Section 5.4.3).

The main conclusions of this section (see Table 5.1 - next page) are

- 1 The regional changes in temperature may vary substantially from the global mean, and the magnitudes of regional changes in precipitation and soil moisture are typically 10 to 20% at 2030 under the IPCC "Business-as-Usual" Scenario.
- 2 Although there is still substantial disagreement in some regions between the models considered, the agreement is better than in earlier studies (e.g., Schlesinger and Mitchell, 1987).

5.4.2 Limitations Of Simulated Regional Changes

Although there is agreement between models on the qualitative nature of the large-scale changes in temperature and to a lesser extent precipitation, there is much less agreement when one considers variations in the changes on

a regional (sub continental) scale (i.e., areas of order 1 000 000 km²). For example, it is likely that increases in greenhouse gases will increase precipitation near 60 degrees of latitude north, but there is little agreement between models on the variation of the increases with longitude. The horizontal resolution of most models used until now (typically 250-700km) is inadequate to produce an accurate representation of many of the regional features of climate, especially precipitation, which is strongly influenced by topography. The parameterization of processes not explicitly resolvable on the model grid also leads to errors at regional scales. The models in Table 3.2a do not allow for changes or interannual variations in oceanic heat transport.

The nature of inter-model discrepancies in these studies is illustrated by considering the changes averaged over several regions of about 4,000 000 km². The regions are chosen so as to represent a range of climates. Different models perform well in different regions. Inconsistencies in the changes produced by different models may be resolved to some extent by selecting those models giving the more realistic simulations of present climate. Such critical evaluations at regional level will best be done by the potential users and revised as improved model simulations become available. Confidence in any one prediction of spatial *variations* in changes at a regional scale must presently be regarded as low.

An estimate of the changes in temperature, precipitation and soil moisture averaged over the 5 regions selected by IPCC is given in Section 5.4.4. The results are based on the high resolution studies (Table 3.2a, entries 20-22) since in general these produce a better simulation of present day climate (see Section 4). Results from five low resolution models (Grotch 1988, 1989, personal communication) (Table 3.2a, entries 3, 7, 11, 13, 15) were also considered. There may be considerable variations within the regions and in the changes produced by the different models within the regions.

5.4.3 Assumptions Made In Deriving Estimates For 2030

The following assumptions have been made

- 1) **The concentrations of greenhouse gases increase as in the IPCC "Business-as-Usual" Scenario.** This assumes only modest increases in efficiency and gives an effective doubling of CO₂ by about 2020 and an effective quadrupling by about 2080. Reference will also be made to IPCC Scenario B which assumes large efficiency increases and substantial emission controls which delay an effective doubling of CO₂ to about 2040.
- ii) **The "best guess" of the magnitude of the global mean equilibrium increase in surface temperature due to doubling CO₂ (the climate sensitivity) is**

Table 5.1 Estimates of changes in areal means of surface air temperature and precipitation over selected regions, from pre-industrial times to 2030 assuming the IPCC "Business-as Usual" Scenario. These are based on three high resolution equilibrium studies which are considered to give the most reliable regional patterns but scaling the simulated values to correspond to a global mean warming of 1.8°C the warming at 2030 assuming the IPCC "best guess" sensitivity of 2.5°C and allowing for the thermal inertia of the oceans. The range of values arises from the use of three different models. For a sensitivity of 1.5°C, the values below should be reduced by 30%, for a sensitivity of 4.5°C they should be increased by 50%. **Confidence in these estimates is low**, particularly for precipitation and soil moisture. Note that there are considerable variations in the changes within some of these regions.

REGION	M O D E L	TEMPERATURE (°C)		PRECIPITATION (% change)		SOIL MOISTURE (% change)	
		DJF	JJA	DJF	JJA	DJF	JJA
1 Central North America (35-50°N, 80-105°W)	1	4	2	0	-5	-10	-15
	2	2	2	15	-5	15	-15
	3	4	3	10	-10	-10	-20
2 South East Asia (5-30°N, 70-105°E)	1	1	1	-5	5	0	5
	2	2	1	0	10	-5	10
	3	2	2	15	15	0	5
3 Sahel (10-20°N, 20W-40°E)	1	2	2	-10	5	0	-5
	2	2	1	-5	5	5	0
	3	1	2	0	0	10	-10
4 Southern Europe (35-50°N, 10W-45°E)	1	2	2	5	-15	0	-15
	2	2	2	10	-5	5	-15
	3	2	3	0	-15	-5	-25
5 Australia (12-45°S, 110-155°E)	1	1	2	15	0	45	5
	2	2	2	5	0	-5	-10
	3	2	2	10	0	5	0

The numbers 1, 2 and 3 in the third column correspond to the models under entries 20, 21 and 22 respectively in Table 3 2a

2.5°C. This estimate is based on evidence from both models and observations (Section 5 2 1)

- iii) **The most reliable estimate of the regional patterns of change is given by the high resolution models.** (Table 3 2a, entries 20-22) These models in general produce a better simulation of present climate than those run at lower resolution (Section 5 4 1) and give results which are more consistent than those from earlier low resolution studies (see for example, Schlesinger and Mitchell 1987 and Section 5 4 4) Note that although other models give a mean warming which is closer to the best guess (for

example, Table 3 2a, entries 17-19) they have a coarser resolution which degrades their simulation of regional climate. Hence the patterns of change have been derived from the high resolution models, even though they give a warming which is larger than the 'best guess' of 2.5°C

- iv) **The patterns of equilibrium and transient climate change are similar.** As stated in Section 5 4 1, the few time dependent simulations that have been run do not use the IPCC Emission Scenarios and so cannot be used directly and have been run at low horizontal resolution degrading their capability to

simulate regional changes. Recent results from the coupled ocean-atmosphere models (Section 6) indicate that the reduction of the warming due to oceanic thermal inertia is particularly pronounced in the circumpolar ocean of the southern ocean and the northern North Atlantic where deep vertical mixing of water occurs. Elsewhere, the reduction is much smaller and the time-dependent response is similar to the equilibrium response (Section 6, Figure 6 5c). The distribution of the changes in the hydrological cycle was also similar to that at equilibrium, but reduced in magnitude.

v) **The regional changes in temperature, precipitation and soil moisture are proportional to the global mean changes in surface temperatures.**

This will be approximately valid except possibly in regions where the changes are associated with a shift in the position of steep gradients, for example where the snowline retreats, or on the edge of a rainbelt which is displaced. In general, this assumption is likely to be less valid for precipitation and soil moisture than for temperature. In the experiment described in detail in Section 6 (Stouffer et al., 1989), the mean temperature response north of 30°S is about 15% higher than the global mean response; this enhancement is omitted in the regional estimates given below.

vi) **The changes in global mean temperature can be derived from a simple diffusion-upwelling box model.** For the Business-as-Usual Scenario, this gives a warming of 1.3 to 2.6°C from pre-industrial times to present, with a "best guess" of 1.8°C (Section 6.6.2). For Scenario B, these estimates should be reduced by about 15%.

Although it is hard to justify some of these assumptions on rigorous scientific grounds, the errors involved are substantially smaller than the uncertainties arising from the threefold range of climate sensitivity. On the basis of the above assumptions, the estimates of regional change have been obtained by scaling the results from the high resolution models by a factor of $1.8/\Delta T_s$ where ΔT_s is the climate sensitivity of the model involved.

5.4.4 Estimates Of Regional Change; Pre-industrial to 2030 (IPCC "Business-as-Usual" Scenario)

The reader should be aware of the limited ability of current climate models to simulate regional climate change and assumptions made in deriving the regional estimates (Sections 5.4.2 and 5.4.3 respectively). The range of values indicates the range of uncertainty in regional changes arising from using three different models with a similar global sensitivity. The results assume a global mean warming of 1.8°C at 2030, consistent with a global mean sensitivity of 2.5°C (Section 6.6.2). IPCC Scenario B gives results which are about 15% lower. For a sensitivity of 1.5°C, the estimates below should be reduced by 30%, for a sensitivity of 4.5°C, they should be increased by 50%. In general, **confidence in these estimates is low**, especially for the changes in precipitation and soil moisture. The regions are shown in Figure 5.13 and the estimates from the three individual models are given in Table 5.1.

Central North America (35-50°N, 85-105°W)

The warming varies from 2 to 4°C in winter and 2 to 3°C in summer. Precipitation increases range from 0 to 15% in winter whereas there are decreases of 5 to 10% in summer. Soil moisture decreases in summer by 15 to 20% of the present value.

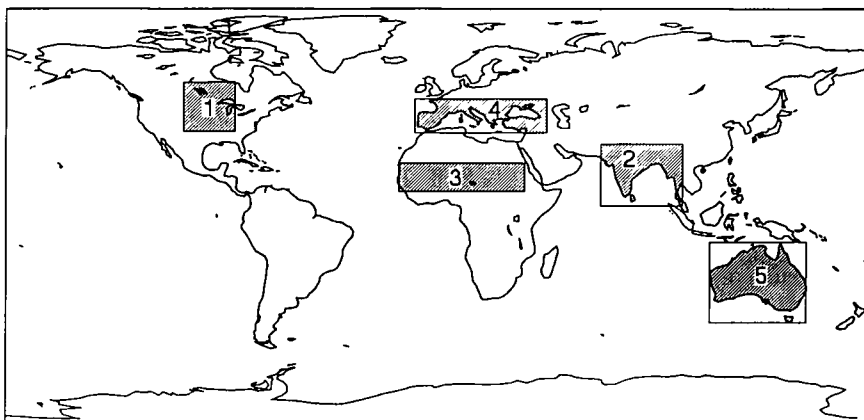


Figure 5.13: IPCC regions for which area means are given in Section 5.4.4 and Table 5.1

South East Asia (5-30°N, 70-105°E)

The warming varies from 1 to 2°C throughout the year. Precipitation changes little in winter and generally increases throughout the region by 5 to 15% in summer. Summer soil moisture increases by 5 to 10%.

Sahel (10-20°N, 20°W-40°E)

The warming ranges from 1 to 2°C. Area mean precipitation increases and area mean soil moisture decreases marginally in summer. However, there are areas of both increase and decrease in both parameters throughout the region which differ from model to model.

Southern Europe (35-50°N, 10°W-45°E)

The warming is about 2°C in winter and varies from 2 to 3°C in summer. There is some indication of increased precipitation in winter, but summer precipitation decreases by 5 to 15%, and summer soil moisture by 15 to 25%.

Australia (10-45°S, 110-155°E)

The warming ranges from 1 to 2°C in summer and is about 2°C in winter. Summer precipitation increases by around 10%, but the models do not produce consistent estimates of the changes in soil moisture. The area averages hide large variations at the sub-continental level.

Many of the differences in these results can be attributed to differences in model resolution, neglect or otherwise of ocean heat transport, and differences in the number of physical processes included and the way they are represented.

5.5 Empirical Climate Forecasting

5.5.1 Introduction

In the light of the poor reliability of regional climate simulations using general circulation models, various authors have suggested the use of data from past climates as indicators of regional climatic relationships for projections of future climate (for example Flohn, 1977; Budyko et al., 1978; Budyko, 1980; Kellogg and Schwere, 1981; Budyko and Izael, 1987; Budyko et al., 1987). A brief description of the method is given in Section 3.4.1.

The mid-Holocene (5-6 kbp), the Last Interglacial (Eemian or Mikiluno, 125-130 kbp) and the Pliocene (3-4 mbp) have been used as analogues for future climates. January, July and mean annual temperatures and mean annual precipitation were reconstructed for each of the above three epochs (see Section 7.2.2). Estimates of the mean temperatures over the Northern Hemisphere exceed the present temperature by approximately 1, 2 and 3-4°C during the mid-Holocene, Eemian and Pliocene respectively. These periods were chosen as analogues of future climate for 2000, 2025 and 2050 respectively.

5.5.2 Results

5.5.2.1 Temperature

Winter-time temperature changes in the low and middle latitude zones are quite small for areas dominated by marine climates. Winter cold is, however, less severe in the interior regions of the continents in middle and high latitudes. Summer warming is greater mainly in high latitudes. In some low latitude continental regions there are some areas of cooling due to increasing evaporation resulting from increased precipitation over these regions.

5.5.2.2 Precipitation

The influence of global warming on annual precipitation over the continents appears to be more complicated than for air temperature. During the mid-Holocene, precipitation was greater than at present over most of the northern continents although there were decreases in some regions of the European territory of the Soviet Union, as well as in some central regions of the United States (Figure 7.4b). Reconstructions of the Pliocene climate indicate that precipitation increased over all land areas for which data are available, particularly in a number of areas that are now deserts (Figure 7.2b). For this epoch, the mean latitudinal increase in annual precipitation over the continents of the Northern Hemisphere seems to show little dependence on latitude, averaging approximately 20 cm yr⁻¹. The tentative results for the Eemian for which data are less complete, indicate that precipitation considerably exceeded the modern value in all regions for which data exist. As discussed in Section 7, the data used in this study have various limitations, and it is possible that the need for datable material to survive has introduced a bias against finding evidence of aridity.

5.5.3 Assessment Of Empirical Forecasts

1. For a climate situation in the past to be a detailed analogue of the likely climate in the next century with increased greenhouse gas concentration it is necessary for the forcing factors (e.g. greenhouse gases, orbital variations) and the boundary conditions (e.g. ice coverage, topography, etc.) to be similar.

The change in forcing during the mid-Holocene and Eemian was very different to that due to doubling CO₂. During both these periods, CO₂ concentrations were smaller than present, being close to the pre-industrial level (Barnola et al., 1987). The orbital perturbations increase the annual mean radiative heating in high latitudes (up to 5 Wm⁻² during the mid-Holocene) and reduce it in the tropics (1 Wm⁻² during the mid-Holocene). The radiative forcing due to doubling CO₂ increases everywhere, from about 2.5 Wm⁻² in high latitudes to 5 Wm⁻² in the tropics (Mitchell, 1990). The changes in orbital perturbations produce seasonal anomalies of up to 40 Wm⁻² at certain latitudes (Berger, 1979) whereas the CO₂ forcing is

relatively constant throughout the year. Thus the mid-Holocene and Eemian cannot be considered as reliable analogues for a climate with increased concentrations of greenhouse gases.

The changes in forcing during the Pliocene are less well known. Carbon dioxide levels may have been higher than present, but whether or not they were as high as double present concentrations is disputed (Section 7.2.2.1). Other factors, such as a lower Himalayan massif and an open Isthmus of Panama (which would have profoundly affected the circulation of the North Atlantic) are likely to have altered the climate in those regions. The geographical distribution of data for the Pliocene are limited and there are difficulties in establishing that data from different sites are synchronous (Section 7.2.2). In view of all these factors, it is at best unclear that the reconstructed patterns of climate change during the Pliocene can be regarded as analogues of warming due to increases in greenhouse gases.

2. Because many aspects of climate change respond to these factors and conditions in a non-linear way, direct comparisons with climate situations for which these conditions do not apply cannot be easily interpreted.

The analogue method is based on the assumptions that the patterns of climate change are relatively insensitive to the different changes in forcing factors leading to warming. Recent numerical studies of the equilibrium response to increased CO₂ give a consistent picture of continental scale changes so one can compare the large-scale features from these simulations with those deduced from the palaeo-analogue approach. The main discrepancies are

i) The palaeo climatic data suggest a cooling over large areas of the tropics whereas CO₂ simulations produce a substantial warming.

A cooling is consistent with the reduction in insolation in the tropics during the mid-Holocene and Eemian, and is also reproduced in numerical simulations in which the orbital perturbations have been imposed (for example, Kutzbach and Guetter 1986, Mitchell et al., 1988). As noted above increases in CO₂ produce a radiative warming of the tropics, whereas the relevant changes in orbital properties produce a radiative cooling. Thus on both simple physical grounds and on the basis of model simulations, the palaeo-climatic reconstructions are probably misleading in this respect.

ii) The palaeo climatic data suggest that precipitation increases markedly in much of the arid subtropics of the Northern Hemisphere (for example COHMAP members 1988, Section 7.2.2.2, 7.2.2.3) whereas recent numerical simulations with enhanced CO₂ indicate little change in these regions.

Thus, numerical simulations of the mid-Holocene and Eemian produce increases in precipitation in much of the arid subtropics because the enhanced summer insolation intensifies the summer monsoon circulations. Again, on simple physical grounds and on the basis of model simulations (for example Kutzbach and Guetter, 1986, Mitchell et al. 1988) it appears that the changes in precipitation in the arid subtropics during these epochs are due to orbital changes.

iii) The palaeo climatic data suggest that the warming (in the Northern Hemisphere) in summer would be greatest in high latitudes whereas in model simulations with increased CO₂ (this section) or orbital perturbations (for example Kutzbach and Guetter 1986, Mitchell et al. 1988) the warming is small in high latitudes in summer.

The simulated changes may be in error (though there is a plausible physical explanation) or the palaeo climatic data have been miscompiled or misinterpreted.

From the above it seems likely that changes in orbital parameters alone can account for much of the changes from present climate found in the mid-Holocene and the Eemian that some of the large scale effects of the orbital perturbations differ from those expected with an increase in trace gases, and therefore that a necessary condition for these periods to be considered as analogues for future climate change is that the effects of orbital variations should be subtracted out. At present, there is no way of doing this apart from using simulated changes.

In conclusion the palaeo analogue approach is unable to give reliable estimates of the equilibrium climatic effect of increases in greenhouse gases as suitable analogues are not available and it is not possible to allow for the deficiencies in the analogues which are available. Nevertheless information on past climates will provide useful data against which to test the performance of climate models when run with appropriate forcing and boundary conditions (See Section 4.10). It should be noted that from the point of view of understanding and testing climate mechanisms and models palaeo climatic data on cool epochs may be just as useful as data on warm epochs. Special attention should be paid to times of relatively rapid climatic change when time-dependent effects and ecosystem responses may more closely resemble those to be expected in the coming century.

5.6 The Climatic Effect of Vegetation Changes

5.6.1 Introduction

In addition to the climatic impacts of increasing greenhouse gases, alteration of vegetation cover by man can modify the climate. For small areas this may result in only local

impacts, but for large areas it may result in important regional climate change, and may impinge upon regions remote from the area of change

The vegetative cover (or lack of it) strongly controls the amount of solar radiative heating absorbed by the land surface by varying the albedo (reflectivity). Heat absorbed by the surface, in addition to heating the soil, provides energy for evaporation and for heating the atmosphere directly (sensible heat). Thus, changes in albedo can strongly affect evaporation and atmospheric heating and so influence the hydrological cycle and atmospheric circulation. Other aspects of vegetation cover, such as aerodynamic roughness, stomatal resistance, canopy moisture capacity and rooting depth can affect the partitioning of incoming solar radiation between evaporation and sensible heat.

There are three climatic regions where vegetation changes may have significant impacts on climate: tropical forests, semi-arid and savannah and boreal forests. The first has received considerable attention and is covered in more detail below and in Section 10. Model studies of degradation of vegetation in the Sahel region of Africa, particularly with regard to changes in albedo and soil moisture availability, have shown that rainfall can be reduced over a wide part of the region (Rowntree and Sangster, 1986). Removal of boreal forests has been shown to delay spring snowmelt slightly by increasing albedo (Thomas, 1987).

5.6.2 Global Mean Effects

1 The net effect of deforestation on global mean climate is likely to be small although the regional impacts may be profound

The conversion of forests to grassland is increasing in the tropics. The current rate of deforestation is estimated to be $0.1 \times 10^6 \text{ km}^2 \text{ yr}^{-1}$ (the total area of tropical forest is about $9 \times 10^6 \text{ km}^2$). Associated with the clearing is a substantial release of CO_2 to the atmosphere (Section 1). The replacement of forest by grassland also increases the reflection of solar radiation to space which tends to cool the climate, but this effect is at present small compared with the warming effect of the accompanying increased CO_2 (see Section 1, 2.2.2, Section 2). The net effect of deforestation is therefore to warm climate. The removal of all the tropical forests could warm the climate by about 0.3°C ³. Alternatively, if 10% of the Earth's land surface

³ Assuming that $13 \times 10^6 \text{ km}^2$ of forest is removed and releases $12.5 \text{ Gt C} / 10^6 \text{ km}^2$ (based on Bolin et al. 1986) with half the resulting CO_2 remaining in the atmosphere. Also it is assumed that deforestation increases the surface albedo by 5% and that only 50% of the insolation at the top of the atmosphere reaches the surface. The climate sensitivity is taken to be 3°C for a doubling of CO_2 .

were afforested in addition to the present cover, a global cooling of 0.2 to 0.4°C would be expected.

5.6.3 Regional Effects: Deforestation Of Amazonia

One of the best studied examples of deforestation is the Amazon Basin. Besides changing net carbon storage in Amazonia, deforestation is affecting the regional energy and water balance. A number of modelling studies have concentrated on the climatic impact that might arise from complete deforestation of South America and, in particular, Amazonia (Henderson-Sellers and Gornitz, 1984, Wilson, 1984, Dickinson and Henderson-Sellers, 1988, Lean and Warrilow 1989, Nobre et al., 1990). The Amazon Basin contains about half of the world's tropical rainforests and plays a significant role in the climate of that region. It is estimated that approximately half of the local rainfall is derived from local evaporation (Salati et al., 1978). The remainder is derived from moisture advected from the surrounding oceans. A major modification of the forest cover could therefore have a significant climatic impact. Reduced evaporation and a general reduction in rainfall, although by variable amounts, was found in most experiments.

1 Total deforestation of the Amazon basin could reduce rainfall locally by 20%

The studies by Lean and Warrilow (1989) and Nobre et al. (1990) show reductions of about 20% in rainfall in simulations in which vegetation parameters for forest were replaced by those for grassland (Figure 5.14). Lean and Warrilow showed that albedo and roughness changes contributed almost equally to the rainfall reduction, although more recent work suggests that the contribution from roughness may have been slightly overestimated.

Nobre et al. suggest that the switch to a more seasonal rainfall regime which they obtained, would prevent forest recovery. A recent experiment (Lean and Rowntree, 1989, personal communication) considered the impact of setting vegetation cover to desert over South America north of 30°S . Albedos similar to those of the most reflective parts of the Sahara were used. Annual rainfall was reduced by 70%. The seasonal change of rainfall (Figure 5.15) became typical of that observed in semi-arid regions such as the Sahel. This would permit the growth of some rainy season vegetation and thus a desert would be unlikely to be maintained over the whole region. However, the results suggest that a widespread deforestation of the South American tropics could lead to an irreversible decline in rainfall and vegetative cover over at least part of the region.

5.7 Uncertainties

Here we summarize the major uncertainties in model predictions.

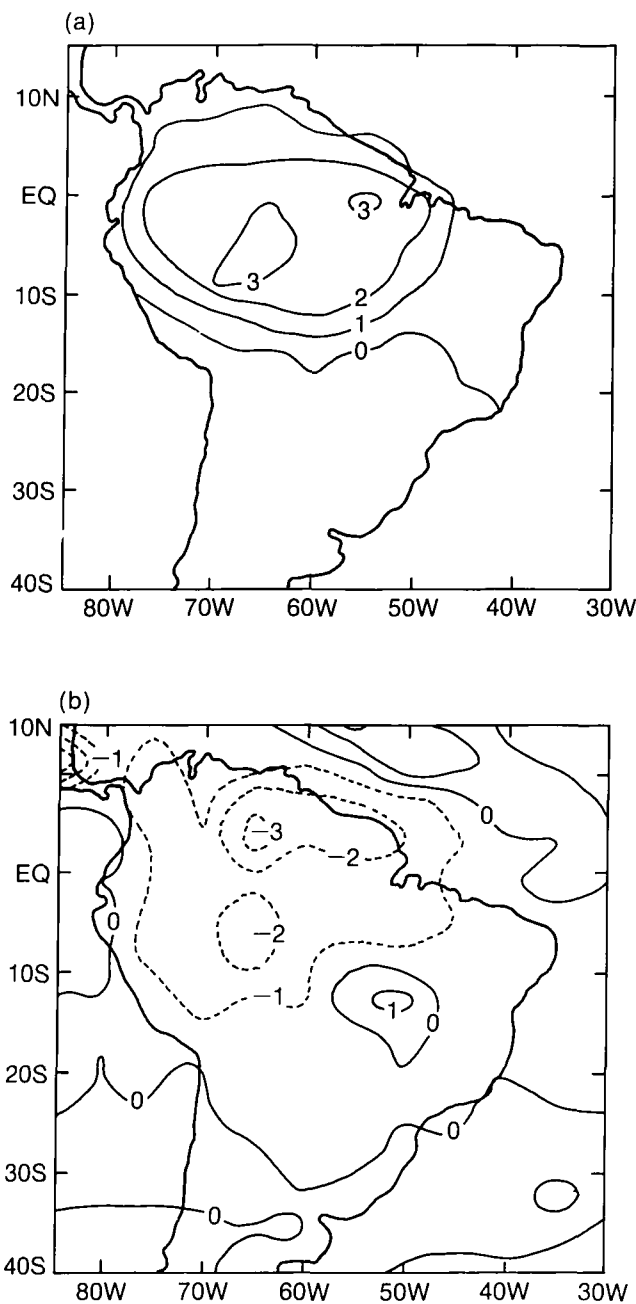


Figure 5.14: Changes in annual means due to deforestation of northern South America (from Nobre et al., 1990) (a) Surface temperature (contours every 1°C), (b) Precipitation (contours every 1 mm day⁻¹, negative contours are dashed)

One of the largest sources of uncertainty in the simulation of equilibrium climate change lies in the prediction of clouds. It has been shown that clouds can produce either a positive or negative feedback depending on the model and parameterization of cloud used (Cess et al., 1989; Mitchell et al., 1989) giving an uncertainty of a factor of two or more in the equilibrium warming. Earlier schemes base cloud cover on relative humidity and

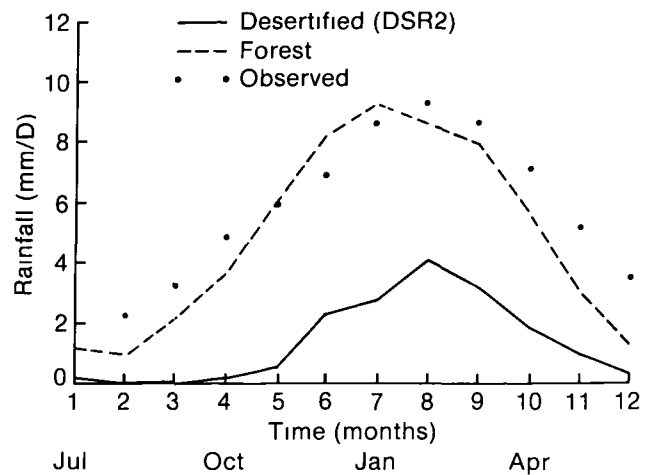


Figure 5.15: Rainfall over South America (2.5 to 30°S, mm day⁻¹) Dashed line simulated, forested surface, Solid line simulated, desert surface Dots, observed (Lean and Rowntree personal communication, 1989)

prescribed radiative properties later models use schemes which explicitly represent cloud water and allow cloud radiative properties to vary. The latter are more detailed but not necessarily more accurate as more parameters have to be specified. The radiative effect of clouds depends on cloud height, thickness and fractional cover, on cloud water content and cloud droplet size distribution (and in the case of ice clouds the size distribution, shape and orientation of particles) (see Section 3.3.4). Thus there is a need to understand both the microphysics of cloud and their relation to the larger scale cloud properties. This will require further satellite observations (for example Barkstrom et al., 1986) and carefully designed field studies (for example Raschke, 1988; Cox et al., 1987). In particular, there is a need to refine our knowledge of ice clouds and their radiative properties.

Another large uncertainty lies in the representation of convection in large-scale models. Again the more detailed (though not necessarily more accurate) parameterizations produce different results from the simpler schemes including a much greater warming in the tropics. It is less obvious how to reduce this uncertainty though it may be that a comparison of the observed and simulated response to past anomalies in tropical SSTs may help to eliminate the more unrealistic schemes.

Thirdly, the changes in ground wetness and surface temperature have been shown to be highly sensitive to the treatment of the land surface. In addition the effects of vegetation and changes in vegetation are ignored in the models used in Table 3.2a. Again process studies along with satellite measurements (World Meteorological

Organization, 1985, 1987) are needed to guide the development of surface parameterizations and their validations.

Finally the oceans and sea-ice constitute a major source of uncertainty about which more is said in Section 6. Here it has been shown that the distribution of sea-ice and changes in sea-ice extent have a dominant influence on local temperature change, especially in winter. Most of the models considered here ignore salinity effects and possible changes in ocean heat and ice transport: some ignore ocean transport altogether. The inclusion of a more complete representation of the ocean may modify the simulated changes in sea-ice described here, and changes in ocean circulation could produce pronounced local anomalies in SST particularly in the neighbourhood of the major current systems or the main areas of deep water formation, with profound effects on the local climate.

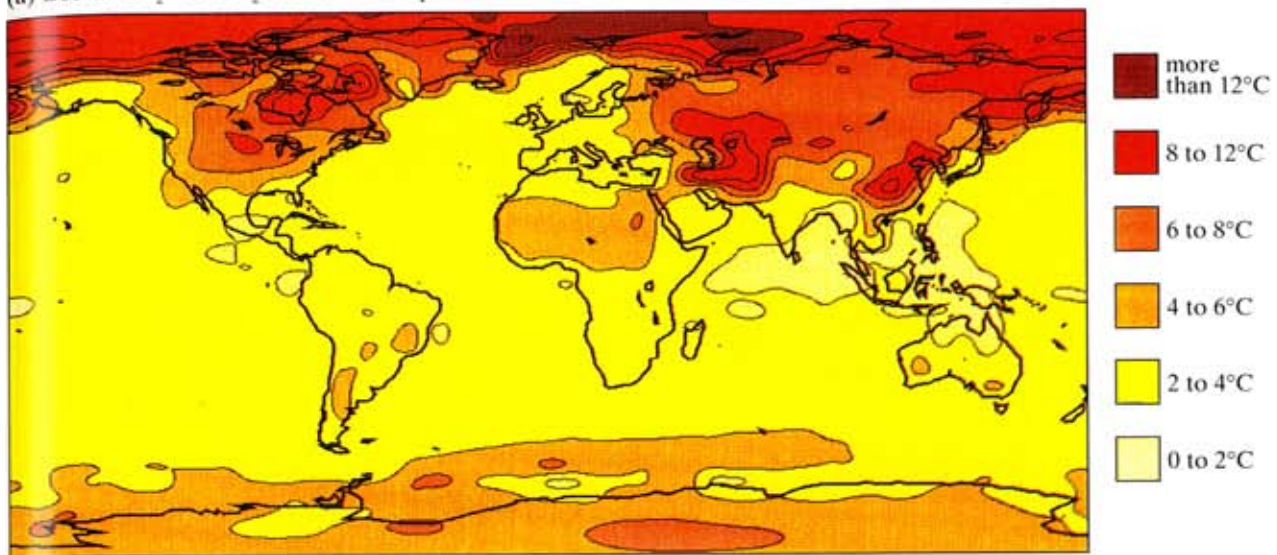
References

- Barkstrom**, B.R. and ERBE Science team, 1986: First data from the Earth Radiation Budget Experiment (ERBE). *Bull. Am. Met. Soc.*, **67**, 818-824.
- Barnola**, J.M., D.Raynaud, Y.S. Korotkevich and C.Lorius, 1987: Vostok ice core provides 160,000-year record of atmospheric CO₂. *Nature*, **329**, 408-413.
- Bates**, G.A. and G.A.Meehl, 1986: The effect of CO₂ concentration on the frequency of blocking in a general circulation model coupled to a simple mixed layer ocean model. *Mon.Wea.Rev.*, **114**, 687-701.
- Bengtsson**, L., H.Bottger and M.Kanamitsu, 1982: Simulation of hurricane type vortices in a general circulation model. *Tellus*, **34**, 440-457.
- Berger**, A., 1979: Insolation signatures of Quaternary climatic changes. *Il Nuovo Cimento*, **20(1)**, 63-87.
- Blackmon**, M., 1975: A climatological spectral study of 500mb geopotential height of the northern hemisphere. *J.Atmos. Sci.*, **37**, 1607-1623.
- Bolin**, B., B.R. Doos, J. Jager and R.A. Warrick (eds), 1986: "The Greenhouse Effect, Climate Change and Ecosystems. SCOPE 13, Wiley, New York.
- Broccoli**, A. and S. Manabe, 1990: Will global warming increase the frequency and intensity of tropical cyclones? (submitted for publication).
- Budyko**, M.I. et al., 1978: "Forthcoming climate change", *Izvestia AN USSR*.
- Budyko**, M.I., 1980: "Climate of the past and future", *Gidrometeorizdat*, 352pp.
- Budyko**, M.I., A.B.Ronov and A.L.Yanshin, 1987: History of the Earth's atmosphere (English translation) Springer-Verlag, Berlin, 139pp.
- Budyko**, M.I. and Y.Izrael, 1987: "Anthropogenic climate change", *Gidrometeorizdat*, 406pp.
- Cess**, R.D. and G.L. Potter, 1988: A Methodology for understanding and Intercomparing atmospheric climate feedback processes in general circulation models. *J. Geophys. Res.*, **93**, 8305-8314.
- Cess**, R.D., G.L. Potter, J.P. Blanchet, G.J. Boer, S.J. Ghan, J.T. Kiehl, H. Le Treut, Z.X. Li, X.Z. Liang, J.F.B. Mitchell, J.J. Morcrette, D.A. Randall, M.R. Riches, E. Roeckner, U. Schlese, A. Slingo, K.E. Taylor, W.M. Washington, R.T. Wetherald, I. Yagai, 1989: Interpretation of cloud-climate feedback as produced by 14 atmospheric general circulation models. *Science*, **245**, 513-516.
- Cox**, S.K., D.S. McDougall, D.A. Randall and R.A.Schiffer, 1987: FIRE (First ISCCP Regional Experiment). *Bull. Am. Met. Soc.*, **68**, 114-118.
- COHMAP** Members, 1988: Climatic changes of the last 18,000 years: Observations and model simulations. *Science*, **241**, 1043-1052.
- Cunnington**, W.M. and J.F.B. Mitchell, 1990: On the dependence of climate sensitivity on convective parametrization. *Climate Dynamics*, **4**, 85-93.
- Dell'Osso**, L. and L.Bengtsson, 1985: Prediction of a typhoon using a finemesh NWP model. *Tellus*, **37A**, 97-105.
- Dickinson**, R.E., 1986: How will climate change? In *The Greenhouse Effect, Climate Change and Ecosystems*, eds. B. Bolin, B.R. Doos, J. Jager and R.A. Warrick, SCOPE 13, Wiley, New York, 206-270.
- Dickinson**, R.E. and A.Henderson-Sellers, 1988: Modelling tropical deforestation: a study of GCM land-surface parametrizations. *Quart.J.R.Met.Soc.*, **114**, 439-462.
- Emanuel**, K.A., 1987: The dependence of hurricane intensity on climate. *Nature*, **326**, 483-485.
- Fels**, S.B., J.D. Mahlman, M.D. Schwarzkopf and R.W. Sinclair, 1980: Stratospheric sensitivity to perturbations in ozone and carbon dioxide: radiative and dynamical response. *J. Atmos. Sci.*, **37**, 2266-2297.
- Flohn**, H., 1977: Climate and energy: A Scenario to the 21st Century. *Climatic Change*, **1**, 5-20.
- Gray**, W.M., 1979: Hurricanes: their formation, structure and likely role in the tropical circulation. In *Meteorology over the tropical oceans* (ed. D.B. Shaw) Roy. Meteor. Soc., 155-218.
- Grotch**, S. L., 1988: Regional intercomparisons of general circulation model predictions and historical climate data. U.S. Dept. of Energy, Washington D.C. Report DOE/NBB-0084 (TR041).
- Hansen**, J., A.Lacis, D. Rind, L. Russell, P. Stone, I. Fung, R. Ruedy and J. Lerner, 1984: Climate Sensitivity Analysis of Feedback Mechanisms. In *Climate Processes and Climate Sensitivity* (ed. J. Hansen and T. Takahashi) Geophysical Monograph 29, 130-163. American Geophysical Union, Washington DC.
- Hansen**, J., D. Rind, A. Delgenio, A. Lacis, S. Lebedeff, M. Prather, R. Ruedy and T. Karl 1989: Regional greenhouse climate effects. In *Coping with climate change*, Proceedings of Second North American Conference on Preparing for climatic change. Dec. 6-8, 1988. Washington DC, pp 696.
- Henderson-Sellers**, A. and V.Gornitz, 1984: Possible climatic impacts of land cover transformations, with particular emphasis on tropical deforestation. *Climatic Change*, **6**, 231-258.
- Ingram**, W.J., C.A. Wilson and J.F.B. Mitchell, 1989: Modelling climate change: an assessment of sea-ice and surface albedo feedbacks. *J. Geophys. Res.*, **94**, 8609-8622.
- Kellogg**, W.W. and R.Schware, 1981: *Climate Change and Society*. Westview Press, Boulder, Colorado.

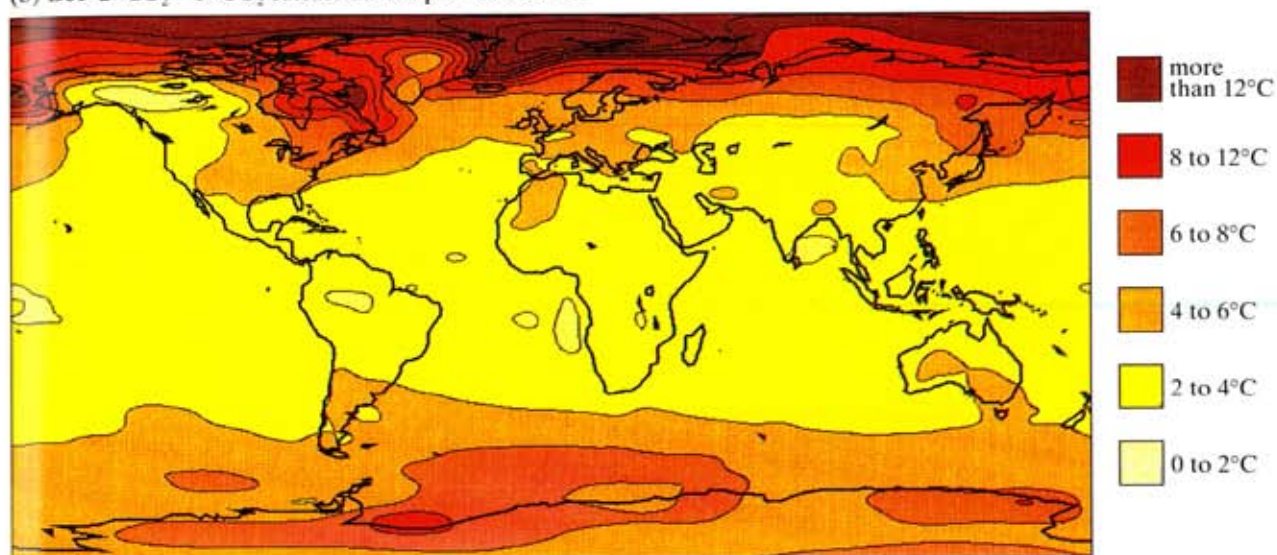
- Krishnamurti, T.N., D. Oosterhof and N. Dignon, 1989:** Hurricane prediction with a high resolution global model. *Mon Wea Rev.*, **117**, 631-669.
- Kutzbach, J.E., and P.J. Guetter, 1986:** The influence of changing orbital parameters and surface boundary conditions on climate simulations for the past 18,000 years. *J Atmos Sci.*, **43**, 1726-1759.
- Lean, J., and D.A. Warrilow, 1989.** Simulation of the regional impact of Amazon deforestation. *Nature*, **342**, 411-413.
- Manabe, S. and R.J. Stouffer, 1980.** Sensitivity of a global climate model to an increase in the CO₂ concentration in the atmosphere. *J Geophys Res.*, **85**, 5529-5554.
- Manabe, S., K. Bryan and M.D. Spelman, 1990:** Transient response of a global ocean-atmosphere model to a doubling of atmospheric carbon dioxide. *J Phys Oceanogr.* (To appear, April).
- Manabe, S. and K. Bryan, 1985:** CO₂ - Induced change in a coupled Ocean-Atmosphere Model and its Palaeo-climatic Implications. *J Geophys Res.*, **90**, C11, 11,689-11,707.
- Manabe, S. and R.T. Wetherald, 1987:** Large scale changes of soil wetness induced by an increase in atmospheric carbon dioxide. *J Atmos Sci.*, **44**, 1211-1235.
- Manabe, S., J.L. Holloway Jr. and H.M. Stone, 1970** Tropical circulation in a time integration of a global model of the atmosphere. *J Atmos Sci.*, **21**, 580-613
- Mearns, L.O., R.W. Katz and S.H. Schneider, 1984:** Extreme high temperature events: changes in their probabilities with changes in mean temperature. *J Clim App Meteorol.*, **23**, 1601-13.
- Mearns, L.O., S.H. Schneider, S.L. Thompson and L.R. McDaniel, 1990:** Analysis of climatic variability in general circulation models: comparison with observations and changes in variability in 2xCO₂ experiments. (submitted for publication)
- Meehl, G.A. and W.M. Washington, 1988:** A comparison of soil moisture sensitivity in two global climate models. *J Atmos Sci.*, **45**, 1476-1492.
- Meehl, G.A. and W.M. Washington, 1989** CO₂ Climate Sensitivity and snow-sea-ice albedo parametrization in an Atmospheric GCM coupled to a Mixed-Layer Ocean Model. *Climatic Change* (to appear).
- Merrill, R.T., 1988:** Environmental influences on hurricane intensification. *J Atmos Sci.*, **45**, 1678-1687.
- Mintz, Y., 1984:** The sensitivity of numerically simulated climates to land-surface boundary conditions. In *The Global Climate* (ed. J.T. Houghton), 79-106, Cambridge University Press.
- Mitchell, J.F.B., 1989:** The "Greenhouse effect" and climate change. *Reviews of Geophysics*, **27**, 115-139.
- Mitchell, J.F.B., 1990:** Greenhouse warming: is the Holocene a good analogue? *J of Climate* (to appear).
- Mitchell, J.F.B. and W.J. Ingram, 1990:** On CO₂ and climate. Mechanisms of changes in cloud. *J of Climate* (submitted).
- Mitchell, J.F.B., N.S. Grahame, and K.J. Needham, 1988:** Climate Simulations for 9000 years before present: Seasonal variations and the effect of the Laurentide Ice Sheet. *J Geophys. Res.*, **93**, 8283-8303.
- Mitchell, J.F.B., C.A. Wilson and W.M. Cunningham, 1987.** On CO₂ climate sensitivity and model dependence of results. *Quart J R Meteorol Soc.*, **113**, 293-322
- Mitchell, J.F.B. and D.A. Warrilow, 1987:** Summer dryness in northern mid-latitudes due to increased CO₂. *Nature*, **330**, 238-240.
- Mitchell, J.F.B., C.A. Senior and W.J. Ingram, 1989.** CO₂ and climate: a missing feedback? *Nature*, **341**, 132-4
- Morris, R.M., 1989:** Forecasting the evolution of tropical storms over the South Indian Oceans and South Pacific during the 1988-9 season using the United Kingdom Meteorological Office operational global model. (unpublished manuscript).
- Nobre, C.J. Shukla, and P. Sellers, 1990:** Amazon Deforestation and Climate Change. *Science*, **247**, 1322-5
- Noda, A. and T. Tokioka, 1989:** The effect of doubling the CO₂ concentration on convective and non-convective precipitation in a general circulation model coupled with a simple mixed layer ocean *J Met Soc Japan*. **67**, 1055-67
- Parry, M.L. and T.R. Carter, 1985:** The effect of climatic variation on agricultural risk. *Climatic Change*, **7**, 95-110.
- Pittock, A.B., 1989:** The greenhouse effect, regional climate change and Australian agriculture. *Proc 5th Agronomy Conf.* Austr. Soc. Agron., Perth, 289-303
- Rashke, E., 1988.** The International Satellite Cloud Climatology Project (ISCCP), and its European regional experiment ICE (International Cirrus Experiment) *Atmos Rev.*, **21**, 191-201
- Raval, A. and V. Ramanathan, 1989:** Observational determination of the greenhouse effect. *Nature*, **342**, 758-761
- Rind, D., R. Goldberg, J. Hansen, C. Rosensweig and R. Ruedy, 1989a,** Potential evapotranspiration and the likelihood of future drought. (Submitted to *J Geophys Res*)
- Rind, D., R. Goldberg and R. Ruedy, 1989b:** Change in climate variability in the 21st century. *Climatic Change*, **14**, 5-37.
- Roeckner, E., U. Schlese, J. Biercamp and P. Loewe, 1987:** Cloud optical depth feedbacks and climate modelling. *Nature*, **329**, 138-139.
- Rowntree, P.R. and A.B. Sangster, 1986:** Remote sensing needs identified in climate model experiments with hydrological and albedo changes in the Sahel. Proc ISLSCP Conference, Rome, European Space Agency ESA SP-248, pp 175-183.
- Salati, E., Marques, J. and L.C.B. Molion, 1978** Origem e Distribuicao das Chuvas na Amazonia. *Interiencia*, **3**, 200-206.
- Schlesinger, M.E., 1985:** Feedback analysis of results from energy balance and radiative-convective models. In *Projecting the climatic effects of increasing atmosphere carbon dioxide*, ed. M.C. MacCracken and F.M. Luther, pp 280-319. US Department of Energy, Washington DC, 1985. (Available as NTIS, DOE ER-0237 from Nat. Tech. Inf. Serv. Springfield Va.)
- Schlesinger, M.E. and J.F.B. Mitchell, 1985:** Model Projection of Equilibrium Climatic Response to Increased CO₂ Concentration. In *Projecting the climatic effects of increasing atmosphere carbon dioxide*, ed. M.C. MacCracken and F.M. Luther, pp 280-319, US Department of Energy, Washington DC, 1985. (Available as NTIS, DOE ER-0237 from Nat. Tech. Inf. Serv. Springfield Va.)

- Schlesinger** M E and J F B Mitchell, 1987 Climate model simulations of the equilibrium climatic response to increased carbon dioxide *Reviews of Geophysics* **25** 760-798
- Siegmund** P, 1990 The effect of doubling CO₂ on the storm tracks in the climate of a GCM K N M I report No 90-01
- Smith** R N B, 1990 A scheme for predicting layer clouds and their water content in a general circulation model *Quart J R Meteorol Soc* **116** 435-460
- Somerville**, R C J and L A Remer, 1984 Cloud Optical Thickness Feedbacks in the CO₂ Climate Problem *J Geophys Res* **89**, 9668-9672
- Somerville**, R C J and S Iacobellis, 1988 Air sea Interactions and Cirrus Cloud feedbacks on climate In Proceedings of the 7th American Meteorological Society Conference on Ocean-atmosphere Interaction, 53-55
- Spelman** M J and S Manabe, 1984 Influence of Oceanic Heat Transport upon the Sensitivity of a model climate *J Geophys Res*, **89**, 571-586
- Stouffer** R J S Manabe and K Bryan, 1989 Interhemispheric asymmetry in climate response to a gradual increase of CO₂ *Nature* **342** 660-662
- Thomas** G, 1987 Land-use change and climate An investigation of climate modelling and climate monitoring techniques PhD thesis, University of Liverpool, UK
- UNEP**, 1989 Report on Scientific Assessment of Stratospheric Ozone
- U.S. National Academy of Sciences**, 1979 Carbon Dioxide and Climate A Scientific Assessment Washington D C pp22
- Vinnikov**, K Ya, and I B Eserkepova, 1989 Empirical data simulations of soil moisture regime *Meteorologia i Gidrologia*, **11**, 64-72
- Wang**, W C, G Y Shi and J T Kiehl 1990 Incorporation of the thermal radiative effect of CH₄, N₂O, CF₂Cl₂ and CFC₁₃ into the Community Climate Model *J Geophys Res* (to appear)
- Washington**, W M and G A Meehl, 1984 Seasonal Cycle Experiment on the Climate Sensitivity due to a doubling of CO₂ with an Atmospheric General Circulation Model coupled to a simple mixed layer ocean model *J Geophys Res*, **89**, 9475-9503
- Washington**, W M and G A Meehl, 1986 General Circulation model CO₂ sensitivity experiments Snow ice albedo parameterizations and globally averaged surface air temperature *Climatic Change*, **8**, 231-241
- Wetherald**, R T and S Manabe 1975 The effect of changing the solar constant on the climate of a general circulation model *J Atmos Sci*, **32**, 2044-2059
- Wetherald**, R T and S Manabe, 1988 Cloud Feedback Processes in a General Circulation Model *J Atmos Sci*, **45**, 1397-1415
- Wigley** T M L, 1985 Climatology impact of extreme events *Nature* **316**, 106-7
- Wigley** T M L and M E Schlesinger, 1985 Analytical solution for the effect of increasing CO₂ on global mean temperature *Nature* **315** 649-652
- Wilson** C A, and J F B Mitchell, 1987a A doubled CO₂ Climate Sensitivity experiment with a GCM including a simple ocean *J Geophys Res* **92** 13315-13343
- Wilson** C A and J F B Mitchell, 1987b Simulated CO₂ induced climate change over western Europe *Climatic Change* **10** 11-42
- Wilson**, M F 1984 The construction and use of land surface information in a general circulation model PhD thesis University of Liverpool, UK
- World Meteorological Organisation**, 1985 Development of the implementation plan for the International Satellite Land Surface Climatology Project (ISLSCP) Phase I (eds H J Bolle and S I Rasool) WCP-94, Geneva
- World Meteorological Organisation**, 1987 Report of the second meeting of the scientific steering group on land surface processes and climate (Toulouse, France, 21-26 May, 1986) WCP-126, Geneva

(a) DJF $2\times\text{CO}_2 - 1\times\text{CO}_2$ surface air temperature: CCC



(b) DJF $2\times\text{CO}_2 - 1\times\text{CO}_2$ surface air temperature: GFHI



(c) DJF $2\times\text{CO}_2 - 1\times\text{CO}_2$ surface air temperature: UKHI

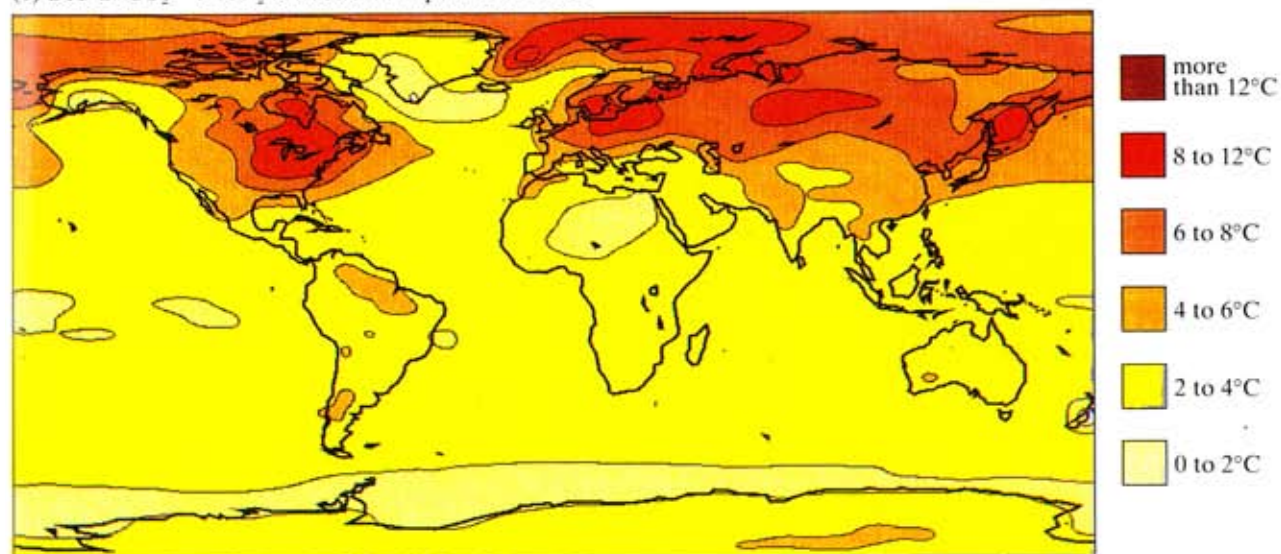
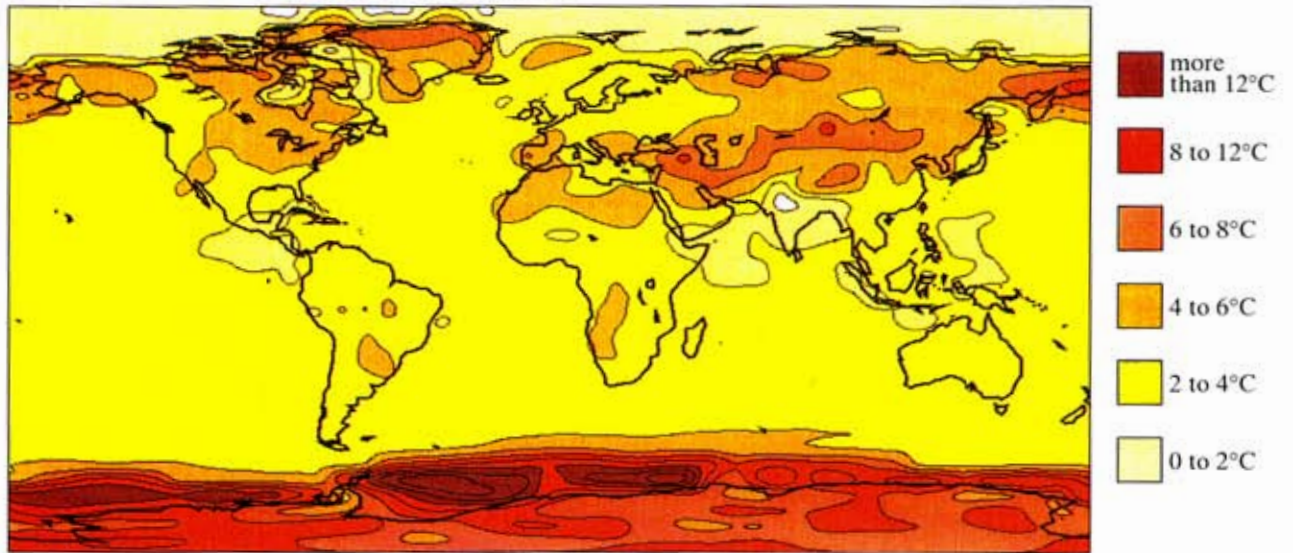
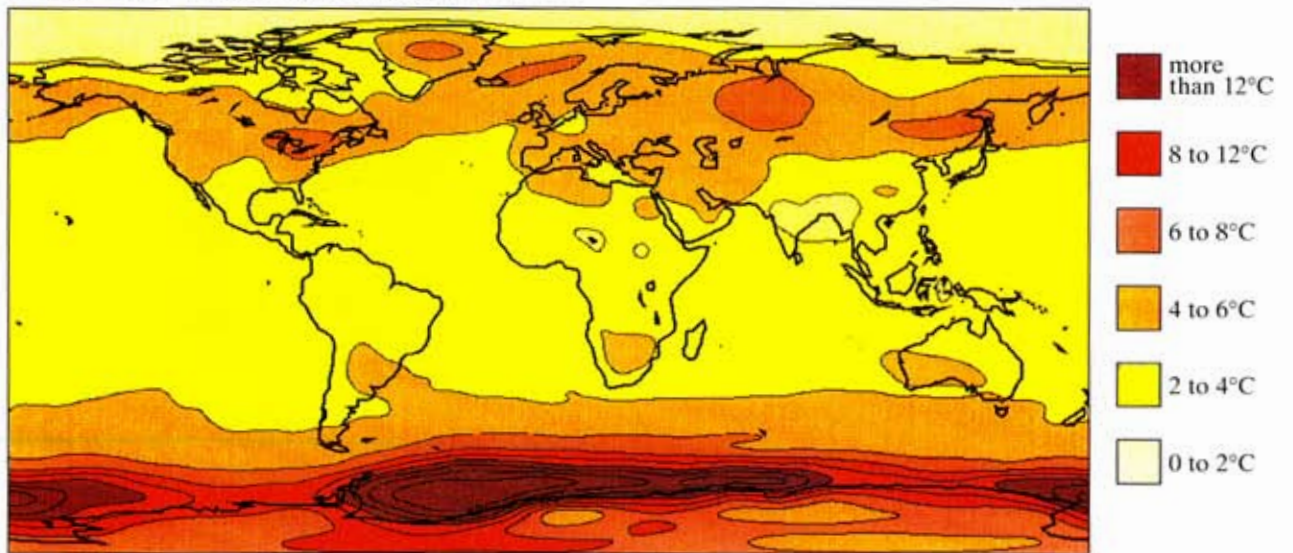


Figure 5.4: Change in surface air temperature (ten year means) due to doubling CO₂, for months December-January-February, as simulated by three high resolution models: (a) CCC: Canadian Climate Centre (Boer, pers. comm., 1989), (b) GFHI: Geophysical Fluids Dynamics Laboratory (Manabe and Wetherald, pers. comm., 1990), and (c) UKHI: United Kingdom Meteorological Office (Mitchell and Senior, pers. comm., 1990). See legend for contour details.

(d) JJA $2\times\text{CO}_2 - 1\times\text{CO}_2$ surface air temperature: CCC



(e) JJA $2\times\text{CO}_2 - 1\times\text{CO}_2$ surface air temperature: GFHI



(f) JJA $2\times\text{CO}_2 - 1\times\text{CO}_2$ surface air temperature: UKHI

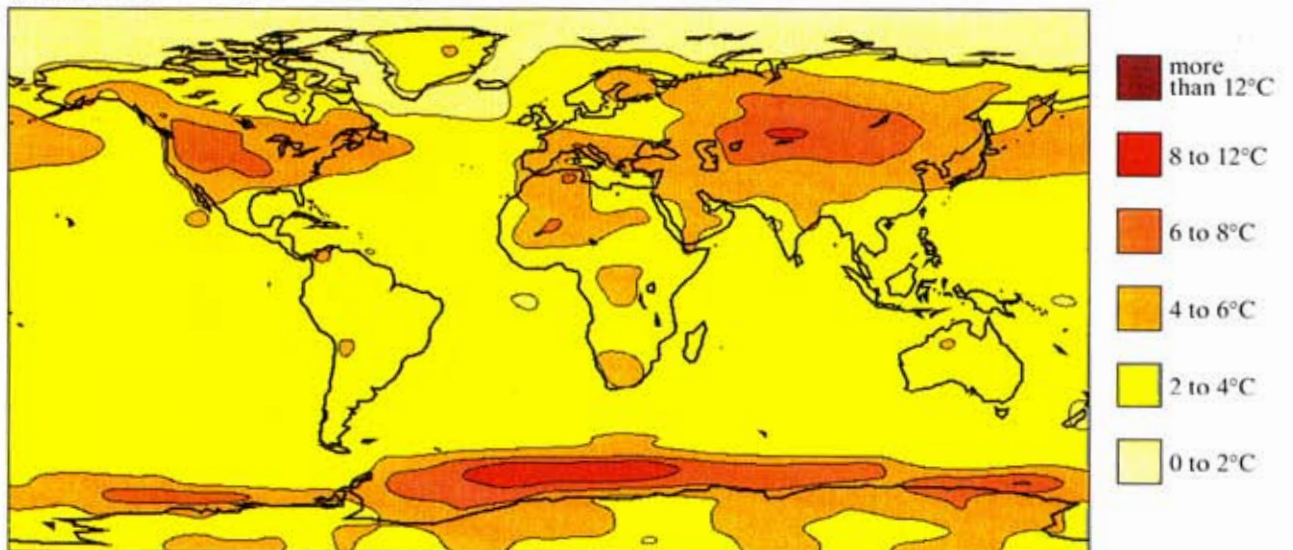
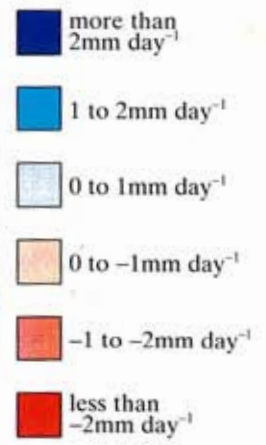
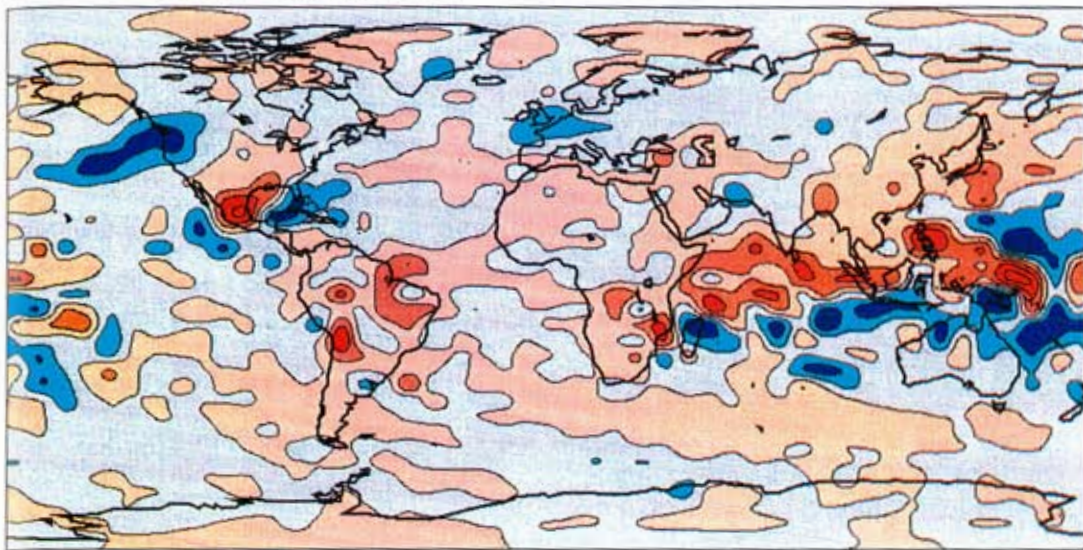
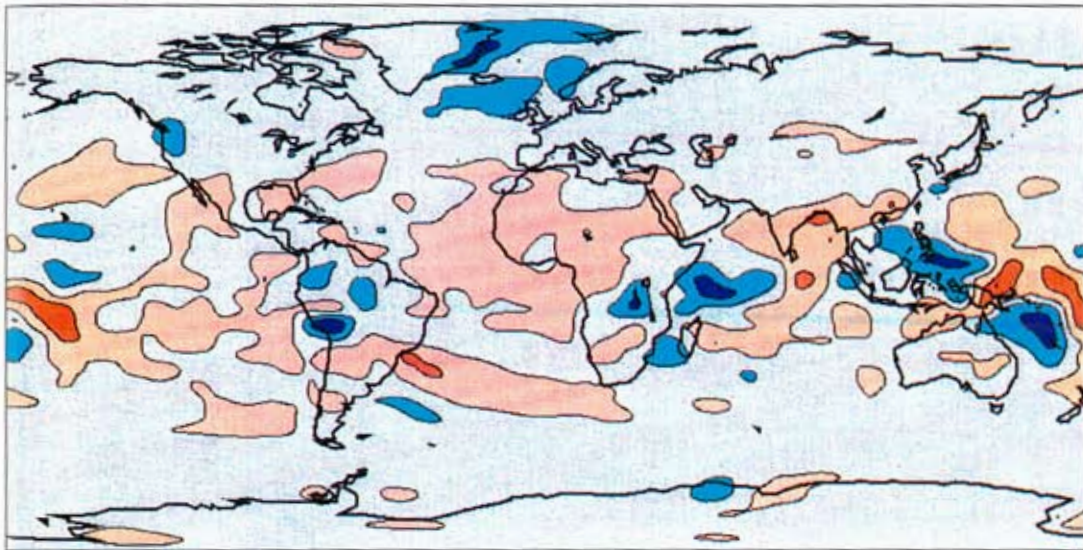


Figure 5.4 continued: Change in surface air temperature (ten year means) due to doubling CO_2 , for months June-July-August, as simulated by three high resolution models: (d) CCC, (e) GFHI, and (f) UKHI. See legend for contour details.

(a) DJF $2\times\text{CO}_2 - 1\times\text{CO}_2$ precipitation: CCC



(b) DJF $2\times\text{CO}_2 - 1\times\text{CO}_2$ precipitation: GFHI



(c) DJF $2\times\text{CO}_2 - 1\times\text{CO}_2$ precipitation: UKHI

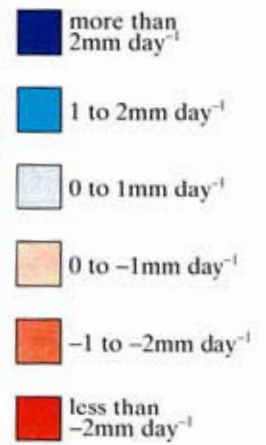
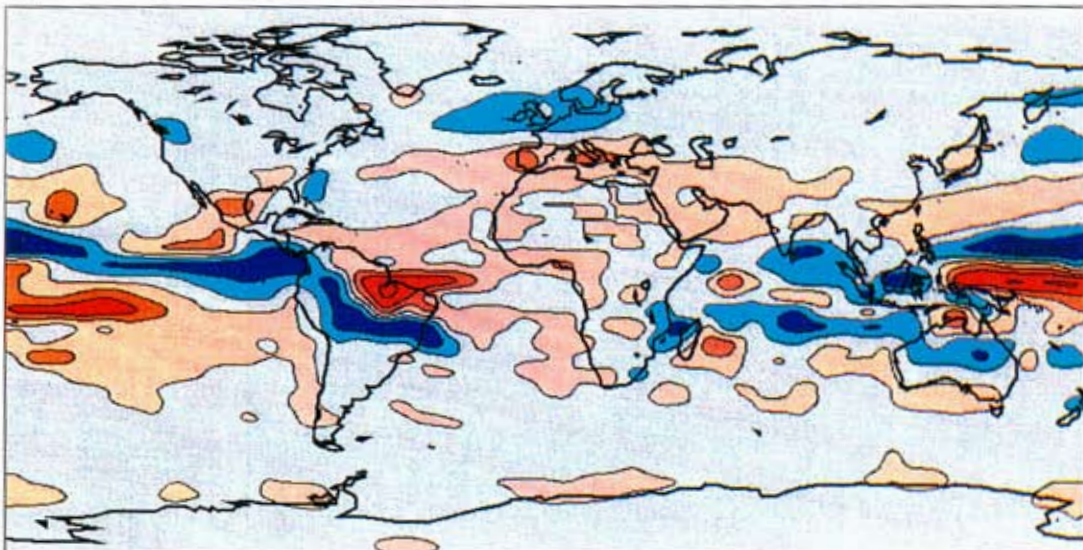
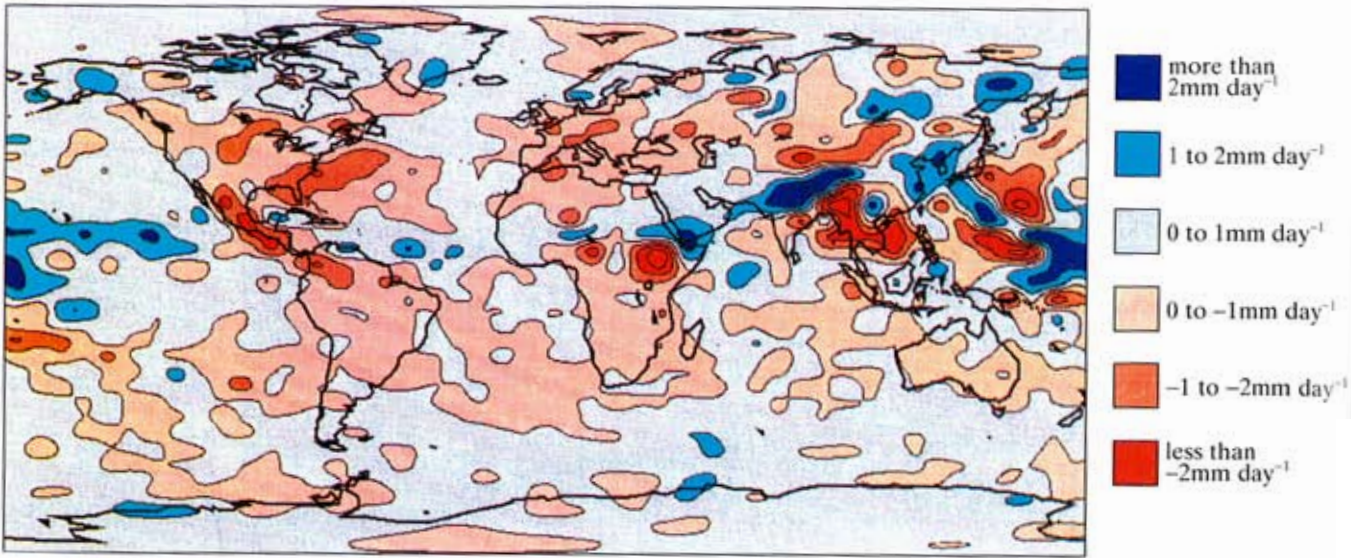
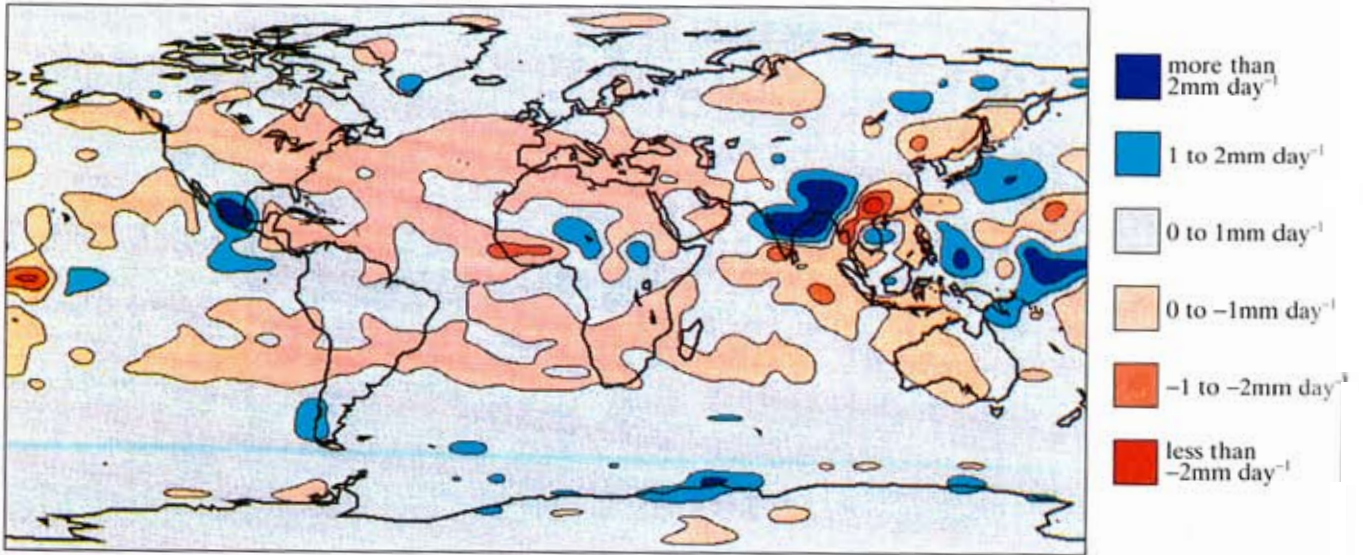


Figure 5.6: Change in precipitation (smoothed 10-year means) due to doubling CO₂, for months December-January-February, as simulated by three high resolution models: (a) CCC, (b) GFHI, and (c) UKHI. See legend for contour details.

(d) JJA $2\times\text{CO}_2 - 1\times\text{CO}_2$ precipitation: CCC



(e) JJA $2\times\text{CO}_2 - 1\times\text{CO}_2$ precipitation: GFHI



(f) JJA $2\times\text{CO}_2 - 1\times\text{CO}_2$ precipitation: UKHI

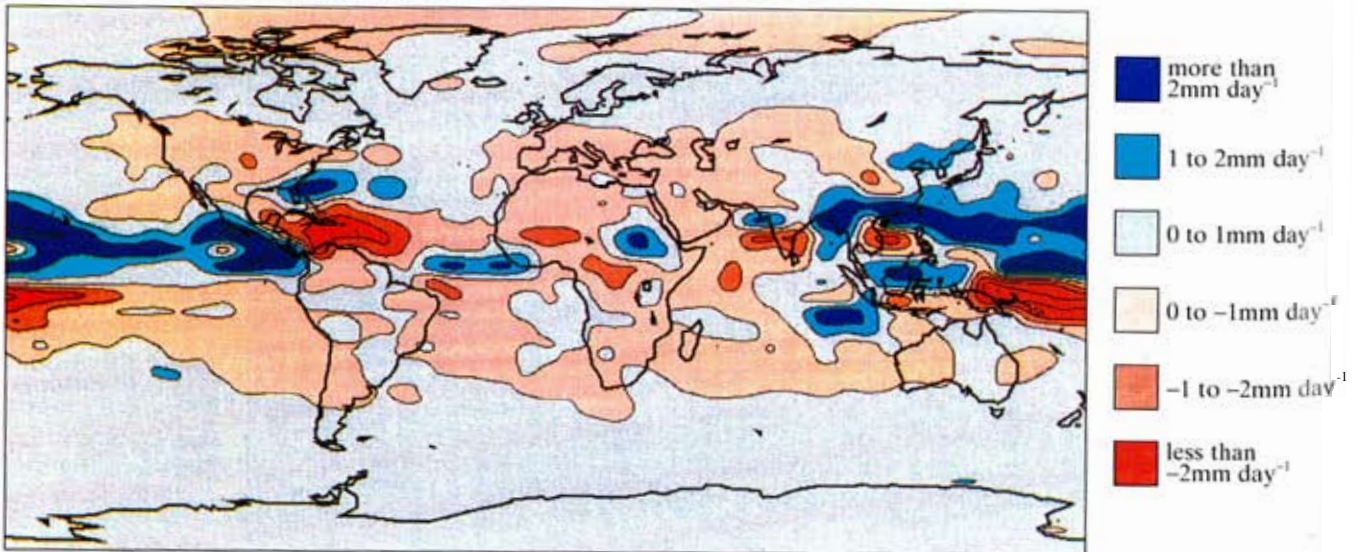
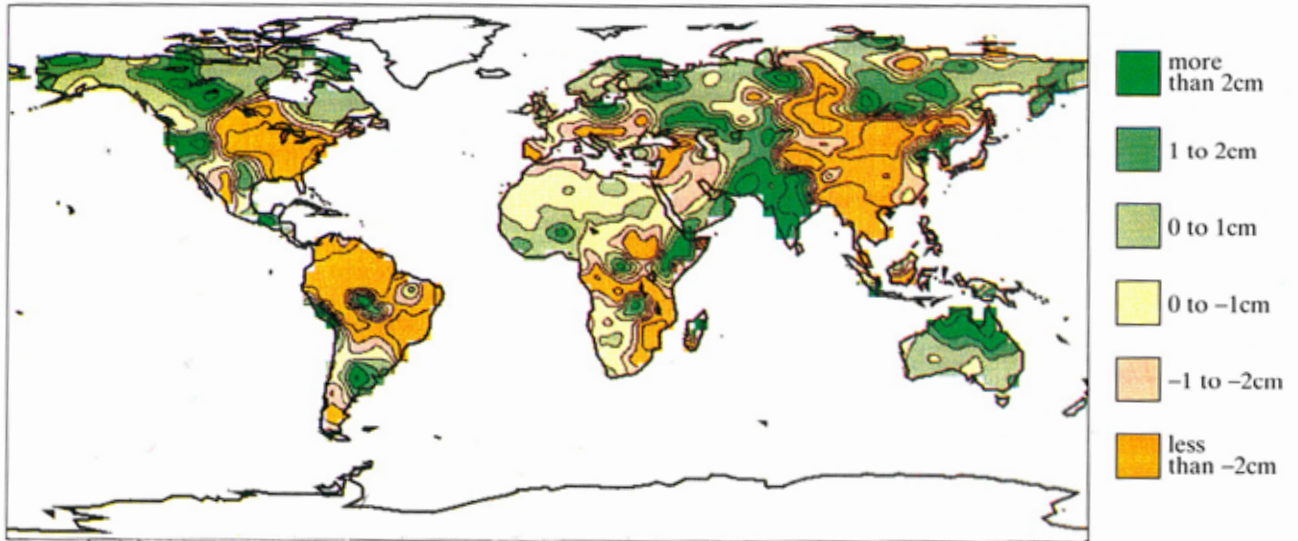
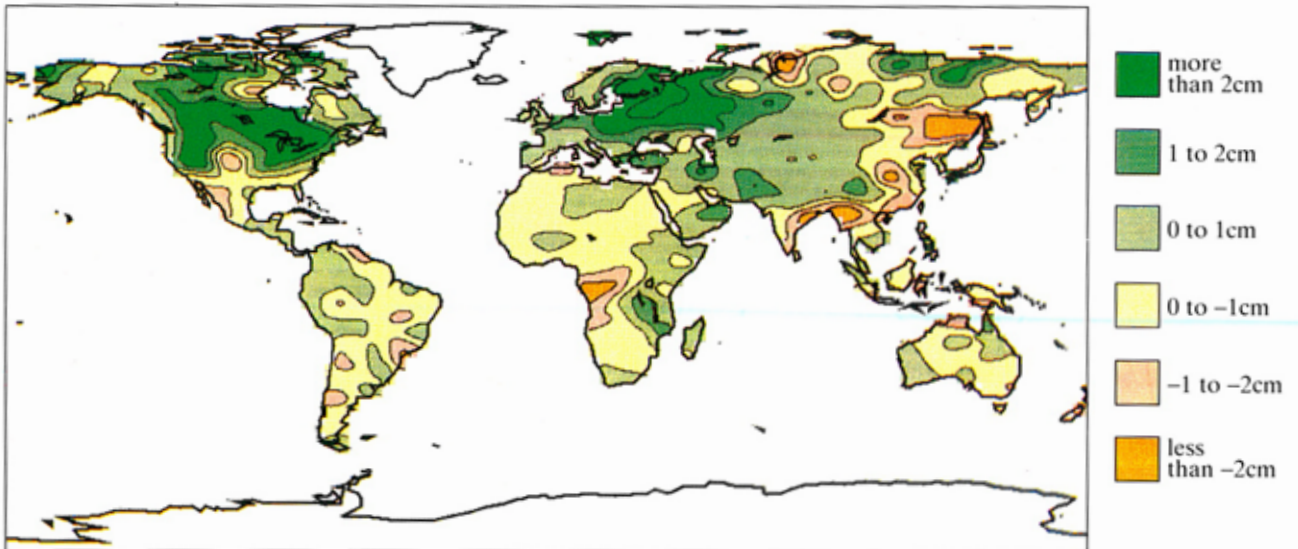


Figure 5.6 continued: Change in precipitation (smoothed 10-year means) due to doubling CO_2 , for months June-July-August, as simulated by three high resolution models: (d) CCC, (e) GFHI, and (f) UKHI. See legend for contour details.

(a) DJF $2\times\text{CO}_2 - 1\times\text{CO}_2$ soil moisture: CCC



(b) DJF $2\times\text{CO}_2 - 1\times\text{CO}_2$ soil moisture: GFHI



(c) DJF $2\times\text{CO}_2 - 1\times\text{CO}_2$ soil moisture: UKHI

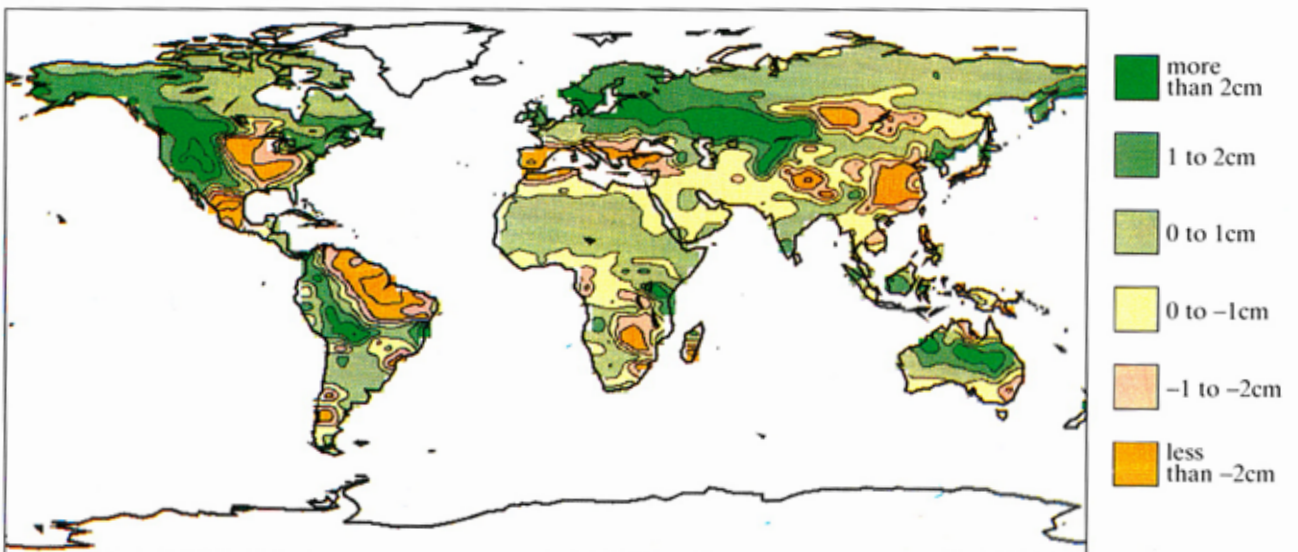
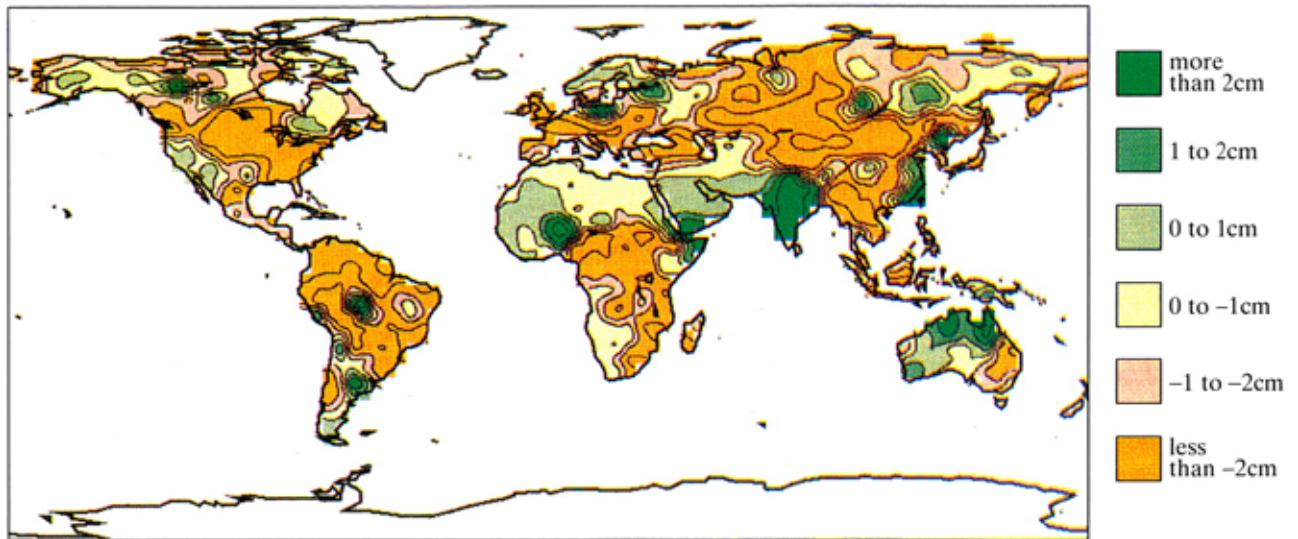
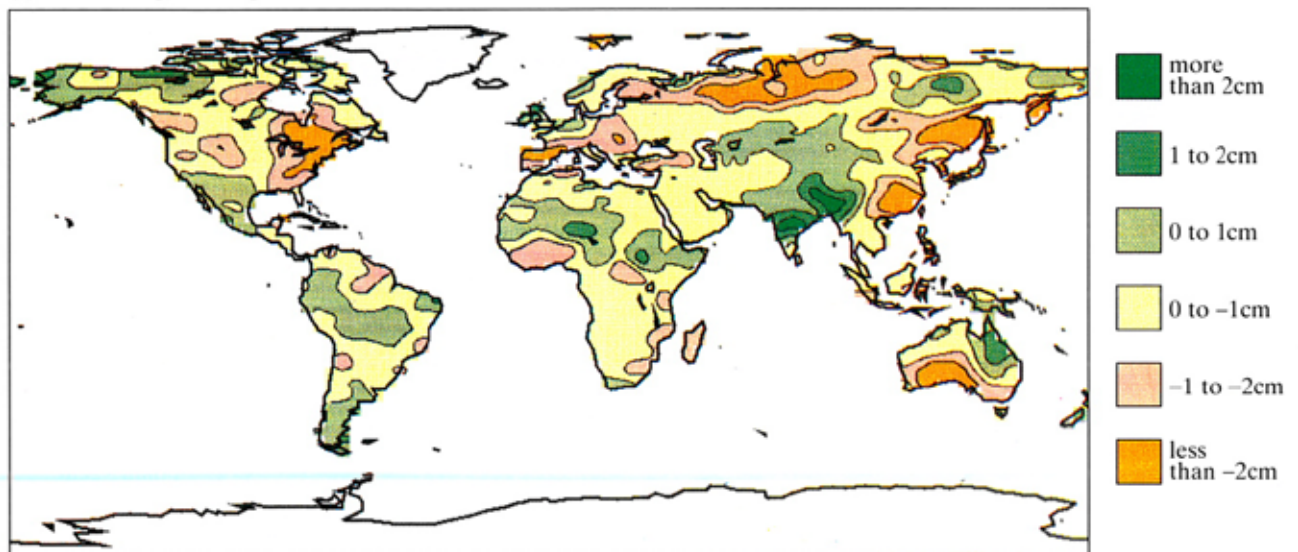


Figure 5.8: Change in soil moisture (smoothed 10-year means) due to doubling CO₂, for months December-January-February, as simulated by three high resolution models: (a) CCC, (b) GFHI, and (c) UKHI. Note that (a) has a geographically variable soil capacity whereas the other two models have the same capacity everywhere. See legend for contour details.

(d) JJA $2\times\text{CO}_2 - 1\times\text{CO}_2$ soil moisture: CCC



(e) JJA $2\times\text{CO}_2 - 1\times\text{CO}_2$ soil moisture: GFHI



(f) JJA $2\times\text{CO}_2 - 1\times\text{CO}_2$ soil moisture: UKHI

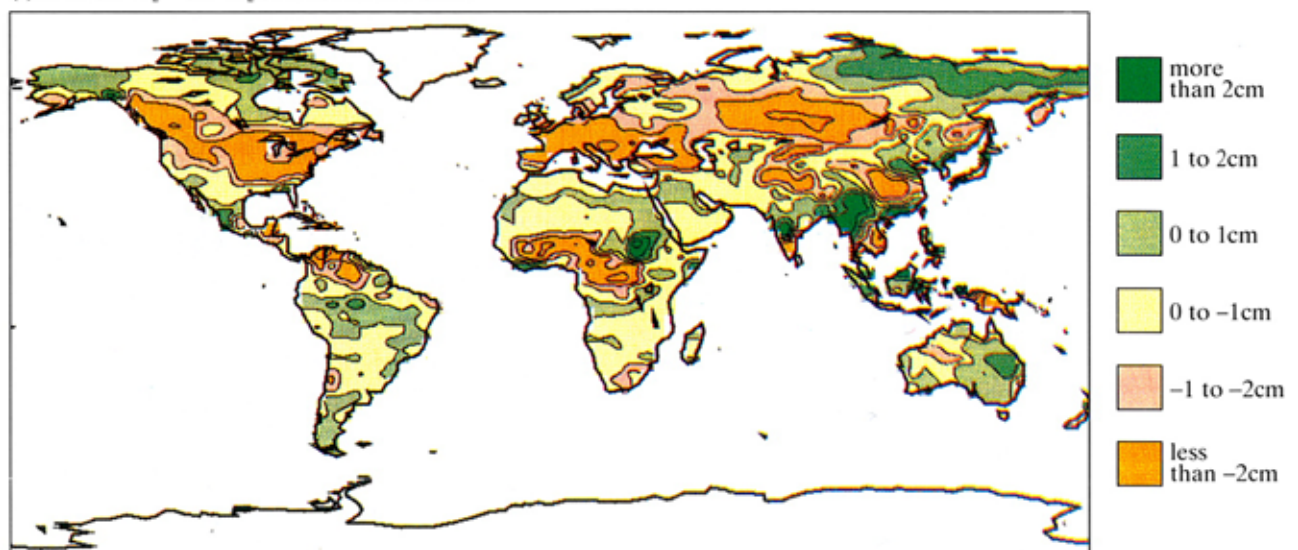
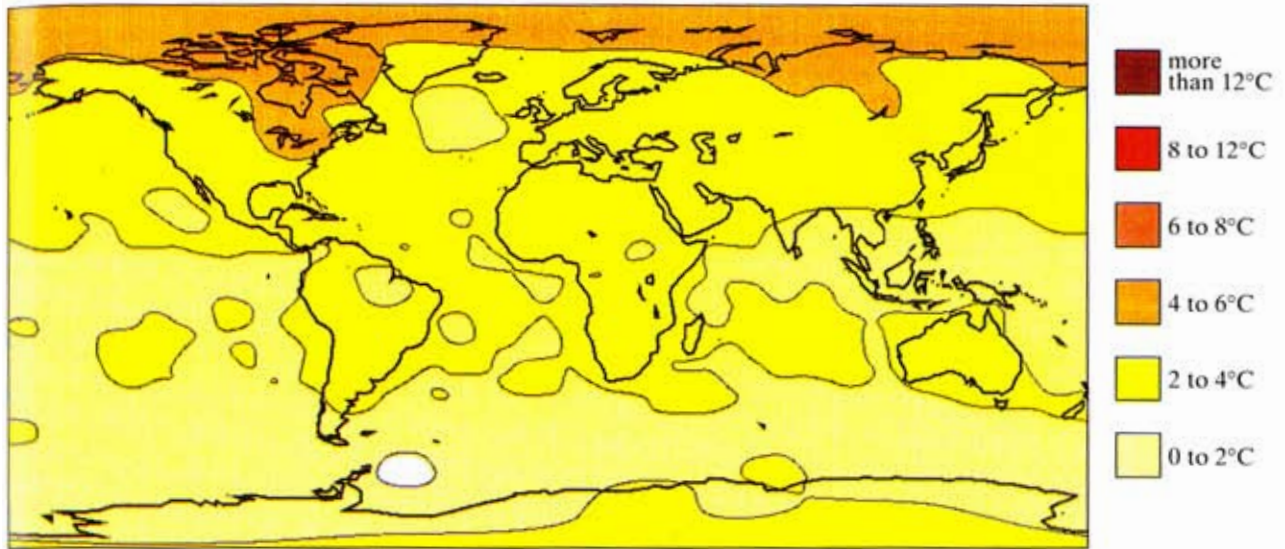
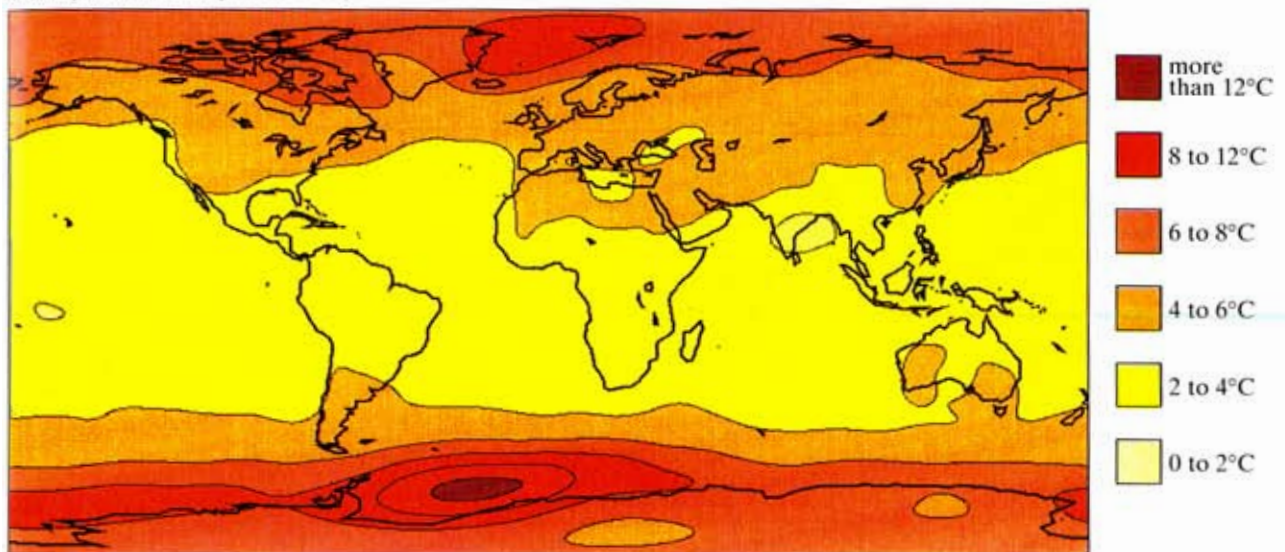


Figure 5.8 continued: Change in soil moisture (smoothed 10-year means) due to doubling CO_2 , for months June-July-August, as simulated by three high resolution models: (d) CCC, (e) GFHI, and (f) UKHI. Note that (d) has a geographically variable soil capacity whereas the other two models have the same capacity everywhere. See legend for contour details.

(a) Years 60-80 of the time-dependent temperature response



(b) Equilibrium temperature response



(c) Ratio of the time-dependent response to equilibrium response

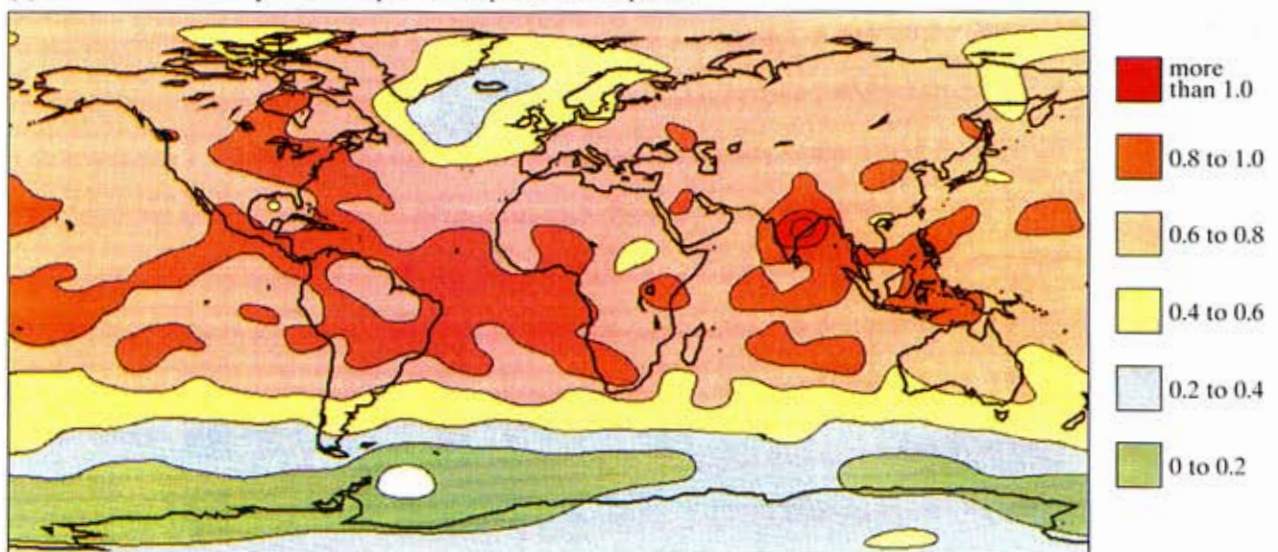
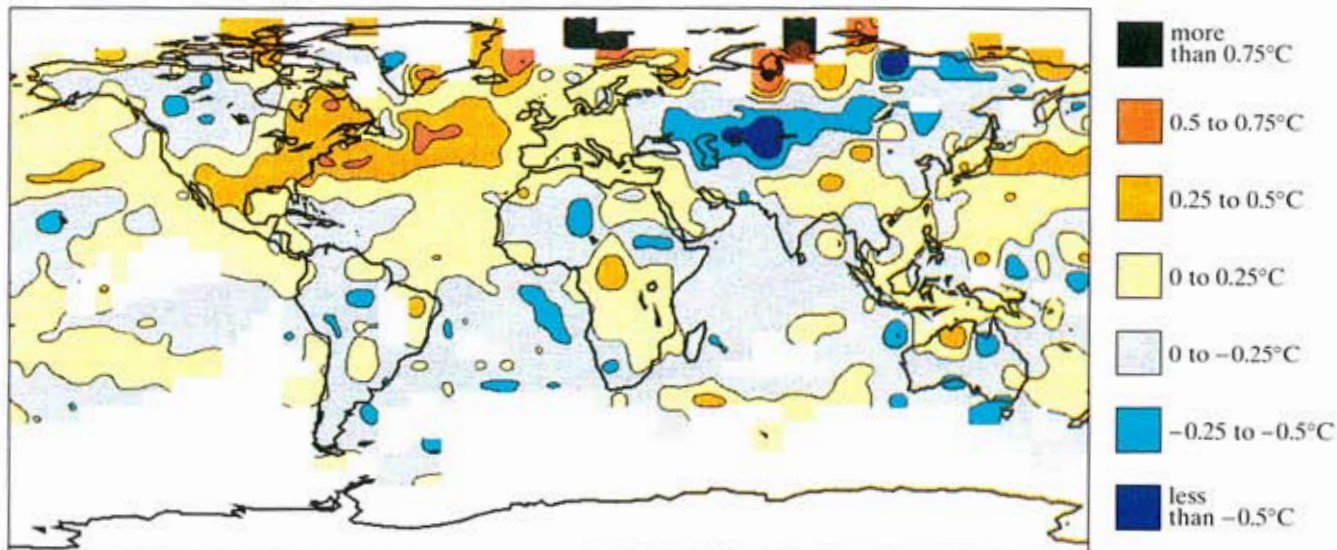
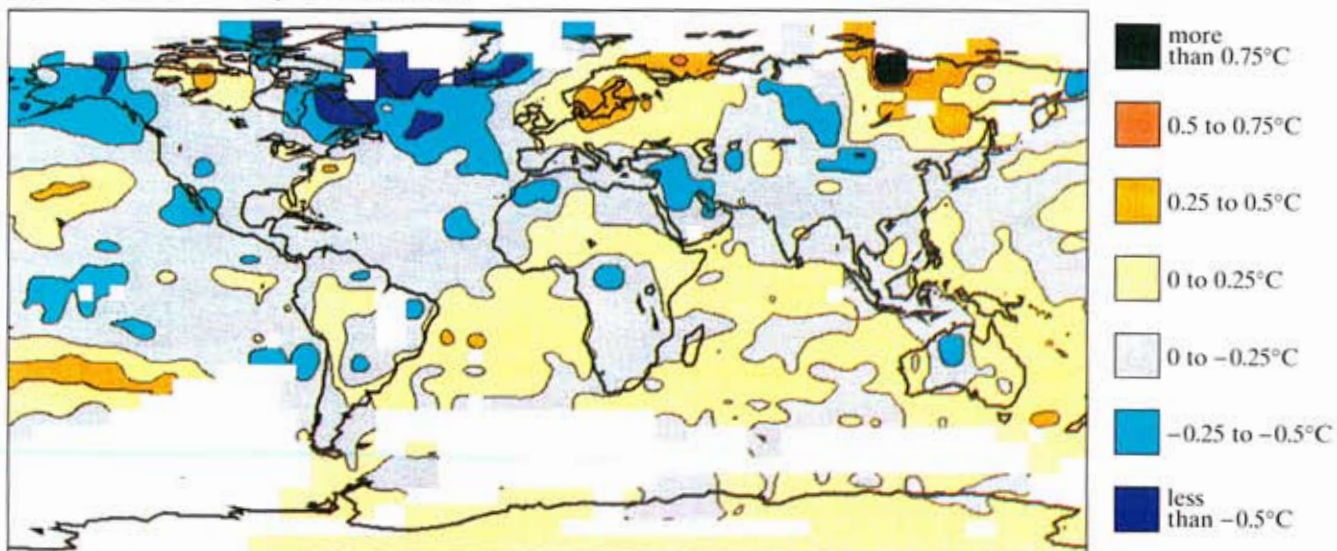


Figure 6.5: (a) The time-dependent response of surface air temperature ($^{\circ}\text{C}$) in the coupled ocean-atmosphere model to a $1\% \text{ yr}^{-1}$ increase of atmospheric CO_2 . The difference between the $1\% \text{ yr}^{-1}$ perturbation run and years 60-80 of the control run when the atmospheric CO_2 concentration approximately doubles is shown. (b) The equilibrium response of surface air temperature ($^{\circ}\text{C}$) in the atmosphere-mixed layer ocean model to a doubling of atmospheric CO_2 . (c) The ratio of the time-dependent to equilibrium responses shown above. From Manabe, pers. comm. (1990). See legends for contour details.

(a) 1950 -1959 surface temperature anomalies



(b) 1967-1976 surface temperature anomalies



(c) 1980 -1989 surface temperature anomalies

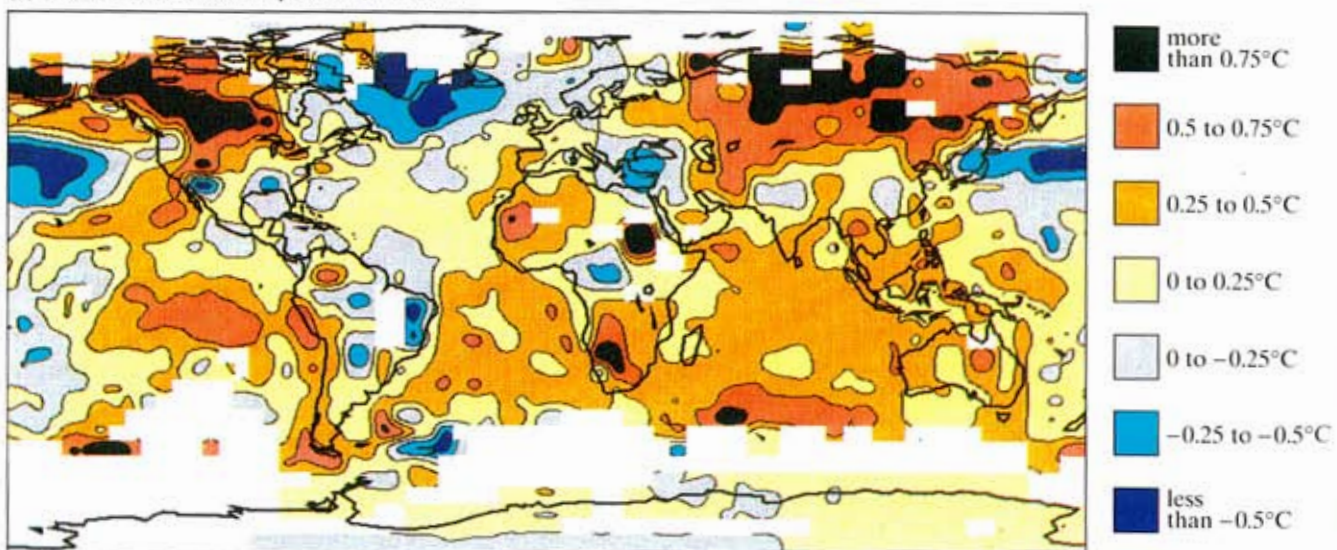


Figure 7.13: Decadal surface temperature anomalies, relative to 1951-80. (a) 1950-1959, (b) 1967-76, (c) 1980-89. Land air temperatures from P.D. Jones and sea surface temperatures from the United Kingdom Meteorological Office. See legend for contour details. White areas show where there are insufficient data.